THE DIAGNOSTIC UTILITY OF INTEGRATION OF DYNAMIC CONTRAST ENHANCED (DCE) AND DYNAMIC SUSCEPTIBILITY CONTRAST (DSC) IN MR PERFUSION PROTOCOLS , IN GRADING AND BIOLOGICAL BEHAVIOUR CHARACTERIZATION OF INTRA-AXIAL BRAIN TUMORS

THESIS SUBMITTED IN PARTIAL FULFILLMENT FOR DEGREE OF

DM (NEUROIMAGING AND INTERVENTIONAL

NEURORADIOLOGY)

(2016- 2018)

OF THE SREE CHITRA TIRUNAL INSTITUTE FOR MEDICAL

SCIENCES AND TECHNOLOGY

TRIVANDRUM, INDIA

Dr. VIRENDER MALIK

DEPARTMENT OF IMAGING SCIENCES AND INTERVENTIONAL RADIOLOGY,

SREE CHITRA TIRUNAL INSTITUTE FOR MEDICAL SCIENCES

AND TECHNOLOGY, TRIVANDRUM, INDIA

SREE CHITRA TIRUNAL INSTITUTE FOR MEDICAL SCIENCES AND TECHNOLOGY, TRIVANDRUM

CERTIFICATE

This is to certify that the work incorporated in this thesis titled

"THE DIAGNOSTIC UTILITY OF INTEGRATION OF DYNAMIC CONTRAST ENHANCED (DCE) AND DYNAMIC SUSCEPTIBILITY CONTRAST (DSC) IN MR PERFUSION PROTOCOLS, IN GRADING AND BIOLOGICAL BEHAVIOUR CHARACTERIZATION OF INTRA-AXIAL BRAIN TUMORS"

has been carried out by Dr. Virender Malik under our supervision and guidance. The work done in connection with this thesis has been carried out by the candidate himself and is genuine.

Dr C Kesavadas
Co-Principal investigator
Professor & HOD
Department of Imaging Sciences and Interventional Radiology,
SCTIMST, Thiruvananthapuram.

Dr Bejoy Thomas	Dr T R Kapilamoorthy	Dr Krishna Kumar K	Dr Deepti A N
Co – investigator	Co – investigator	Co – investigator	Co- investigator
Professor	Professor	Professor	Asso.Professor
ISIR	ISIR	Neurosurgery	Pathology

DECLARATION

I hereby declare that this thesis titled "the diagnostic utility of integration of dynamic contrast enhanced (DCE) and dynamic susceptibility contrast (DSC) in MR perfusion protocols , in grading and biological behaviour characterization of intraaxial brain tumors" has been prepared by me under the supervision and guidance of Dr. C Kesavadas (Professor & HOD), Dr.Bejoy Thomas (Professor), Dr. T.R *Kapilamoorthy (Professor), Dr. Krishna Kumar (Professor) and Dr Deepti (Associate professor) Sree Chitra Institute for Medical Sciences and Technology, Trivandrum.*

Date: (Dr Virender Malik)

Place: Thiruvananthapuram

ACKNOWLEDGEMENT

- *I am deeply indebted to my teachers and guides Dr. C. Kesavadas , Dr. Bejoy Thomas, Dr. T R Kapilamoorthy , Dr. Krishna Kumar K and Dr Deepti A N for their constant unwavering support, insightful criticism, expert supervision and immense patience throughout this study.*

- *I would especially like to acknowledge my gratitude to my past and present colleagues and the technologists in the department for their valuable assistance at all times.*

- *I would also like to extend my heartfelt gratitude to my son (Aryaman Malik), wife (Dr Abha Kumari) and my parents (Shri Bhagat Singh and Smt kamla Devi), for being immensely supportive and patient all through my endeavors. I could not have achieved a fraction of what I have without their prayers, love, and support.*

- *Finally yet importantly, I am eternally grateful to all my patients & their relatives who have been very understanding and generous with their cooperation all through the study.*

Dr. Virender Malik

Senior Resident,

Dept of IS & IR,

SCTISMT,

Thiruvananthapuram, India

CONTENTS

Introduction

INTRODUCTION:

Dynamic susceptibility contrast (DSC) and dynamic contrast enhanced (DCE) MR perfusion study the different perfusion parameters in brain tumors.

DSC technique has been the most widely used perfusion method till date to measure brain perfusion in brain tumors with rCBV being the most robust and widely used parameter. However, few disadvantages of this first pass bolus technique include the difficulty in determining absolute quantification & permeability assessment , presence of susceptibility artefacts and the invalid assumption of BBB integrity in DSC imaging.[1] DCE MR perfusion, also referred to as "permeability" MRI or " T1 perfusion" , more accurately measure vessel permeability and the extravascular-extracellular space. The increased permeability of newly formed microvessels may accurately correspond with the maximal K-trans and Ve values.[1] So these T1 perfusion parameters application can lead to more accurate glioma grading.

There is marked spatial heterogeneity in high grade glioma and the DCE and DSC perfusion study the different perfusion parameters . Therefore, the integration of both types of perfusion into the protocols, can give a more complete assessment of brain tumor, compared to DCE or DSC MRI perfusion used alone.[2] Such integration of the perfusion parameters, specially without any additional contrast dose being administered, appears a more pragmatic approach in more reliable grading, non-invasive follow up and treatment response of gliomas.

Both perfusion sequences can be performed in a single MRI protocol, with the DCE sequence performed before the DSC sequence. The first injection will serve two functions: first as a preload of gadolinium-based contrast agent to help compensate for

leakage correction for DSC imaging and, second, to provide dynamic data for calculation of permeability metrics.[2]

This study is designed to evaluate the role of combined DSC and DCE MR perfusion in more accurately grading and biological behavior characterisation of brain tumors. Such integration of the perfusion parameters, specially without any additional contrast dose being administered , appears a more pragmatic approach in more reliable grading and non-invasive follow up of brain tumors.

Aims & Objectives

AIMS AND OBJECTIVES

Hypothesis : As there is marked heterogeneity in high grade glioma, and the DCE and DSC MR perfusion study the different perfusion parameters, the integration of both types of perfusion into the protocols, can give a more complete assessment of brain tumor, compared to DCE or DSC MRI perfusion used alone.

Objective : To investigate the diagnostic utility of integration of DCE and DSC into MR perfusion protocols , in grading and biological behavior characterization of brain tumors."

Review of Literature

REVIEW OF LITERATURE

What's the real need of MR Perfusion?

MRI is unambiguously the modality of choice for characterization of brain tumors, providing an exquisite details of the morphological features.[3] However, the lack of functional information (tumour's physiology and biology) with the conventional MR sequences warrants inclusion of advanced MR techniques like MR perfusion for the holistic assessment of a brain tumour.[4,5]

The characterization of tumour grade, more importantly differentiating low grade (WHO I-II) & high grade (WHO III-IV) gliomas, is crucial for decision-making about the mode of treatment. The conventional MRI appearances in enhancing malignant brain tumours (HGN, PCNSL and metastases) may be similar and not indicate a specific diagnosis. Advanced MR imaging plays a crucial role in non-invasive assessment of intra-axial brain masses and aid in making treatment decisions.[6]

The prognostic determination and decision of selecting an optimal therapeutic strategy for glial tumors was exclusively based on histologic grading, till the recent 2016 update on brain tumor classification. Though the integrated layer based diagnosis is the presently advocated mode for considering the individualized treatment, the accurate assignation of histological grade and therefore the importance of a representative sample can't be overemphasized.[7] However, the presence of histologically heterogeneous nature of the high grade glioma is a major hindrance to obtaining a true representative sample and thence to assigning accurate histologic grading.

Considering the later, image guided biopsy is being increasingly used to obtain a true representative sample and avoid inappropriate classification. Targeting enhancing areas

to obtain representative sample has proved useful, however, areas with most dedifferentiation are not necessarily the most enhancing areas.

Contrast-enhancement is usually directly related to the progressively increasing grade of tumour (most GBMs show enhancement), and presence of enhancement in grade II tumours being associated with poorer outcome.[8,9] The glioma in the elderly may show subtle or no enhancement, despite being of high grade.[10]

The parametric values such as rCBV (DSC derived) and K-trans (DCE derived) represent neoangiogenesis and permeability respectively and correlate to areas of most histologic dedifferentiation. The areas with most enhancement and maximum MR perfusion derived parametric values are not necessarily the same and therefore , targeting areas with maximum rCBV and K-trans would yield a better representative sample in comparison to areas with maximum enhancement in such situations.[11]

Can biopsy be avoided ? Feasibility of noninvasive imaging-based tumor grading:

Given the good correlation between MR perfusion derived parameters and the histologic grading, invasive nature of biopsy and the inherent sampling errors (especially with stereotactic biopsy), the acceptance of MR based tumor grading and avoiding the later is pragmatic in certain clinical scenarios.[12]

MR perfusion : options available

The MRI perfusion parameters can be obtained with or without administration of an exogenous contrast agent. The later technique utilizes the magnetically labeled arterial blood water as the endogenous diffusible flow tracer in arterial spin labeling (ASL). The techniques employing administration of an exogenous contrast agent are termed as dynamic susceptibility contrast-enhanced (DSC) or dynamic contrast-enhanced (DCE)

MR perfusion, with the former based on susceptibility and the later on relaxivity effects of administered gadolinium-based contrast agents.[13]

Given the large amount of published work showing strong correlation between tumor grade and the CBV , robust acquisition protocol & analysis technique, the role of DSC MR perfusion in grading gliomas and patient prognostication is acceptable to most authors. However, the published work relating to role of DCE MR perfusion in glioma grading is relatively naïve and is on increase over last decade.[11]

The DSC MR perfusion technique is by far the most common MR perfusion technique in use for glioma grading presently . DSC perfusion techniques utilizes the information processed based on the susceptibility variations that occur during first pass of the contrast bolus through the capillary bed. Though being of undoubtful usefulness in glioma grading , the limitations encountered with this technique include its relative qualitative nature (non absolute quantification parameter) , sensitivity to magnetic field inhomogeneities , rCBV underestimation due to contrast leakage effects, propensity for falsely high rCBV values in setting of cortical based tumor (due to large cortical vessels in tumor proximity) and necessity of high contrast infusion rate for optimal results.[12]

The first pass of contrast agent measures only the permeability in first pass, which is different from permeability measured in the steady state, where measurement of bidirectional exchange between interchanging compartments (plasma and extravascular, extracellular space) can be characterized.[1]

The differences between these two contrast based MR perfusion techniques is summarised in Table 1.

Parameters	DCE	DSC
Physics basis	Relaxivity	Susceptibility
TR (sec)	<0.5 sec	<2 sec
TE (msec)	<10	30 to 40 msec
FA (Flip angle)	20 to 25	60 to 90
Scan time	5 min	2 min
Temporal R	Low	High
Spatial R	High	Low
Measured values	K-trans, Ve, Vp, Kep	rCBV
perfusion absolute quantification	Yes	No (relative)
Susceptibility artifacts	Less	More
Cortical tumors	useful	Useful, inaccurate values d/t proximity to large cortical vessels

Table 1

MR perfusion Parameters : what they depict ?

rCBV (relative cerebral blood volume):

rCBV is the most commonly employed MR perfusion parameter , represents the volume of blood in a given amount of brain tissue (ml of blood / 100 g of brain tissue) and is calculated by assessing the area under the concentration-time curve following contrast administration.[14] Due to recirculation of contrast and presence of capillary permeability,

the cerebral blood volume obtained is only relative and not absolute. Therefore, rCBV value of MR perfusion parameter obtained with DSC perfusion depicts values relative to an internal control (the contralateral normal white matter).

K-trans : Also called as volume transfer constant in unit time , represents the transfer of contrast medium from the vessel into extravascular extracellular space (EES), reflecting the intratumoral microvascular permeability. The increased expression of vascular endothelial growth factor (VEGF) by the high-grade tumors promotes endothelial proliferation, proportion of immature vessels and consequently the endothelial permeability.[15] The K-trans depends on both the blood flow (F) and permeability surface area (PS). However considering the technically difficulty for estimation of these two factors separately and also the expected increase of both with increasing tumor grade**,** the increasing K-trans by itself is expected to be related to tumor grade.[16]

Ve (volume of the extravascular extracellular space) : represents the volume fraction of contrast medium leaking into the EES and can be expressed mathematically as ratio of contrast agent quantity that leaked into EES to the contrast agent quantity that returned to the plasma space.[16]

Although defined as vide supra, the true physiological meaning of Ve remains debatable with various terminologies used to describe this parameter ("leakage space", extravascular extracellular space or its volume or interstitial volume). Considering the variable results showing poor correlation between Ve and cellularity, many authors suggest that Ve provides independent information about microenvironment of tumor. The latter is aptly described in CNS lymphoma which characteristically demonstrate contradictory findings (high Ve as well as high cellularity) and warrants further studies to assess true meaning of Ve.

Vp (plasma volume) :

This parameter represents plasma volume , is derived from DCE acquisition using modified Tofts and Kermode's model.[17,18] It is considered to be closely related to tumor neoangiogenesis. The characteristics of the MR perfusion parameters is summarised in table 2.

Parameter	Unit	Remarks
qCBV	ml/ 100 g	
rCBV	No units	Most studied & used parameter
K-trans	1/min	Depend on Blood flow and permeability surface area Intratumoral microvascular permeability Higher grades→Increased K-trans Correlate with ITSS, MVD, VD
Ve	No units	Close relationship b/w K-trans and Ve values Higher grades→Increased Ve True physiological meaning remains debatable
Vp	No units	Plasma volume Neoangiogenesis

Table 2

Blood brain barrier (BBB) and Neurovascular unit (NVU)

The blood brain barrier(BBB) is characterized by the endothelial cell lining, tight junctions, structural and functional support provided by the astrocytes, microglial cells, pericytes and the continuous basement membranes.[19,20] The interplay of these varied cellular and acellular elements form the so called 'neurovascular unit' (NVU). The NVU gets activated in response to pathogenic stimulus (ex hypoxia), as noted in high grade tumors leading to BBB breakdown.

Imaging translation of BBB disruption in DCE / Why signal increase in DCE perfusion?

The functional integrity of BBB can be ascertained using DCE-MRI in brain pathologies causing its disruption , as in high grade brain tumors.[21] The extravasation of low-molecular weight (LMW) MRI contrast agents following BBB disruption and its consequent accumulation in the EES leads to significantly increased longitudinal relaxation and, therefore the signal intensity in T1-weighted images. The DCE-MRI exploits these characteristics, measures signal enhancement as a function of time and thus evaluate regions of BBB disruption

Multifactorial dependence of DCE perfusion parameters:

Although, the early research in DCE-MRI assumed a linear relationship between contrast uptake and the resultant signal enhancement, its dependence on multiple factors was unarguably agreed subsequently.[22,23] The MR field strength, pre-contrast longitudinal relaxation time of tissue , patient hematocrit**,** type of contrast agent, MR sequence, duration & temporal resolution during data collection following contrast injection , AIF assessment method and the type of pharmacokinetic model applied are among the important factors on which the obtained parametric values (ex k-trans) relies upon.

The different contrast agent demonstrate varying degree of longitudinal and transverse relaxivities and therefore the dose as well as the different type of MR contrast agent used can lead to variance in the obtained parametric values in different DCE-MRI studies.[22] The technique most frequently employed for DCE-MRI is a spoiled gradient echo sequence and its ultra-fast variants.[24] The other less commonly used protocols include other gradient recalled echo sequences and spin-echo methods. The newly

introduced methods include dual-temporal resolution scanning methods and combined and consecutive DSC- and DCE-MRI measurement .[25-28] The importance of calculating pre-contrast longitudinal relaxation time (T10) in individual tissues has been highlighted to negate one of the confounding factors for obtaining accurate DSC derived parametric values.[23,29] The variable flip angle method which employs different flip angles to obtain precontrast datasets is one such method aimed at obtaining exact baseline tissue T1 values prior to the contrast administration.[11,30] The other technique used to obtain T10 is variable saturation time delay, albeit used less frequently compared to the former.

The determination of AIF is an important consideration for reliable measurement of pharmacokinetic parameters. Despite being susceptible to in-flow and partial volume artifacts, the direct measurement of AIF is generally preferred over standard or averaged AIFs.[31] No consensus exist over manual ROI selection or automatic vessel detection with most authors agreeing to optimal method varying according to study aims, pathology and clinical requirements.[24,32] Optimal voxel selection using automatic AIF detection method is based on multiple factors viz. early bolus arrival, a steep wash-in slope, large maximum peak concentration and large area under curve.[32] Using the Arterial Input Functions Obtained from DSC MR Imaging demonstrated higher reliability than AIFDCE-derived PK parameters in Differentiation of High-Grade from Low-Grade Astrocytoma with plausible explanation being larger degree of signal change in DSC-MRI (compared to DCE-MRI) and also introduction of unwanted T2* effects due to increased concentration of the gadolinium- based contrast agent during DCE MR imaging.[33] Some authors have used measurements of AIF from the superior sagittal sinus with acceptable results.[11]

Disagreement exists on whether to use standard hematocrit value or to determine it separately for each patient undergoing DCE-MRI, with the former method being employed in most studies.[24, 34]

Another common assumption is of fast water exchange between compartments with influence of restricted water exchange highlighted in literature, however, receiving little attention during pharamacomodel planning and assigning for a particular study.

The studies pertaining to DCE-MRI reveal markedly varying duration of data collection following contrast injection, with as low as 2.1 min to 155 min.[27] The higher temporal resolution and increased overall scanning time result in more accurate K-trans and Ve values respectively, contrary to underestimation of these parameters while the overall scanning time and temporal resolution are reduced.[35] Considering the longer acquisition time as one of the important reasons to less acceptance of DCE-MRI in clinical practice, Takashi Abe et al in their study utilizing short acquisition time confirmed comparable diagnostic performance to previous studies with longer acquisition times.[36]

Studies based on first-pass pharmacokinetic model (FPPM) analysis , another technique focusing on reduction in the acquisition time for DCE-MRI, concluded that K-trans and Vp values obtained by this method are comparable to obtained using conventional PK model analysis but with major limitation being inability to accurately calculate Ve and therefore justified techniques utilizing longer acquisition to obtain accurate Ve.[37]

The methods analyzing DCE-MRI data, range from fairly simple visual assessment of the enhancement curves to complex pharmacokinetic models. The former provides semi-quantitative measures of BBB breakdown, as the time to maximum enhancement and area under curve (AUC), is easy to obtain but difficult to interpret.[38] The later,

though complex ,provide truly quantitative parameters as k-trans ,ve, kep and Vp and therefore is considered superior in terms of accuracy and physiologically relevance.

The authors are in agreement about selecting an appropriate pharmacokinetic model for obtaining optimal parametric values.[35, 39, 40]

PK modeling was first introduced for DCE-MRI analysis in early 1990s by Brix et al. (1991), and Tofts[41] a consensus 1999 paper on notation[16] with subsequent development of more complex pharmacokinetic models following advances in technology and better understanding of underlying physiology.[24,34] The Conventional Tofts model assumes negligible blood volume (contrast agent in capillaries can be neglected) and a two way transport. This model therefore is valid only in poorly vascularized tissues.[41]

The Modified Tofts model assumes non-negligible blood compartment and a two way transport. This model therefore is valid only in well vascularized tissues.[16]

Patlak model assumes non-negligible plasma compartment and one-way transport of contrast agent. For the Modified Tofts model and the Patlak model, K-trans equal to PS may be assumed for any solution fitting the data well with a non-negligible vp (Fig 1) . So, the Patlak or extended Tofts models would be appropriate in situation with well vascularized tissues (high plasma flow).

A one-way model (e.g. Patlak) may be more appropriate in conditions with slower BBB leakage & short DCE-MRI acquisition duration. In a similar way, applying a two-compartment models to situations with suboptimal temporal resolution is undesired.[34]The use of Akaike information criteria to assess the most suitable model in a particular situation is considered valuable.[24,42]

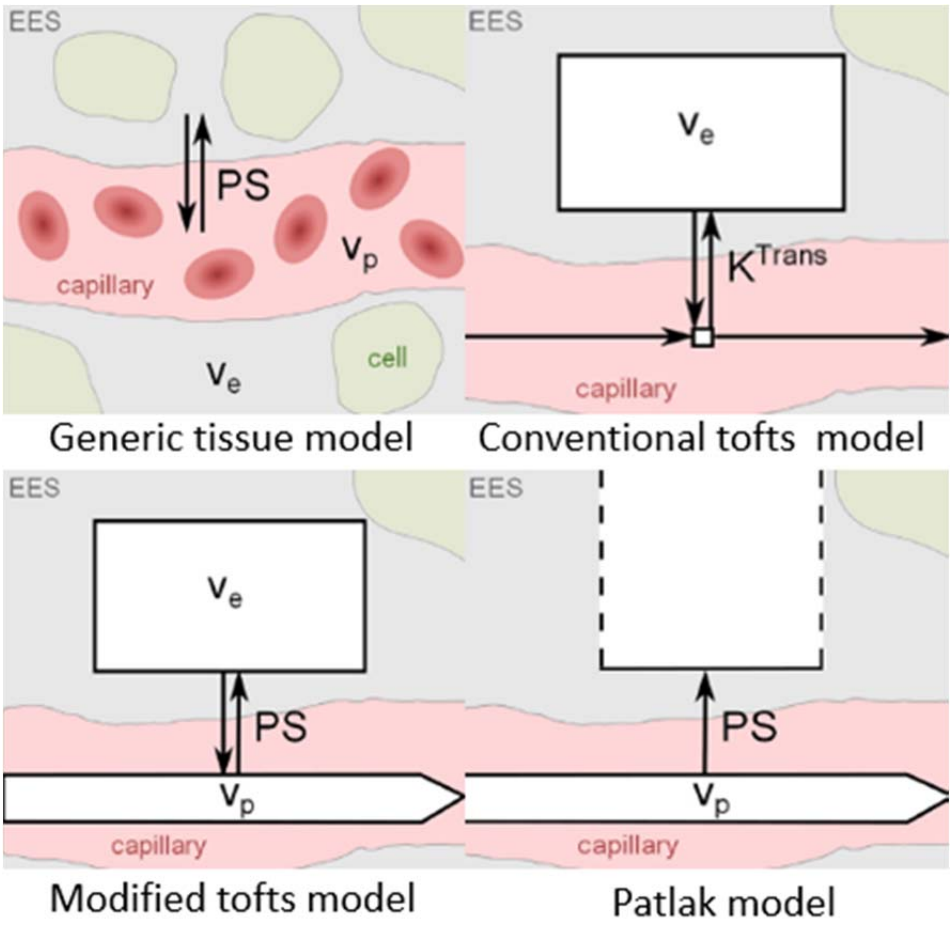

Fig 1

EES: Extravascular extracellular space, Ve: volume fraction, K-trans : transfer constant

Vp: plasma flow , PS : permeability surface area product

DSC perfusion measures T2/T2* signal intensity in the brain tissue and the rCBV parameter obtained plays a key role in differential diagnosis of intra-axial brain masses.[43,44] Lesions with high rCBV distinguishes tumour from non-tumour, corresponds to higher tumour grade, worse prognosis, increased microvessel density and directs biopsy sites with an increased likelihood of obtaining the highest-grade portion of tumour.[44,45] Studies have consistently documented significantly lower rCBV in infectious lesions compared to metastases or high grade glioma.[46-48] Floriano VH et al concluded that rCBV cut-off value of 1.3 differentiated infectious from neoplastic

lesions with sensitivity, specificity and accuracy of 97.8%, 92.6 % and 95% respectively.[46] Despite the usually higher rCBV in neoplasms, the potential for overlap does exist between non-neoplastic lesions and low-grade tumours.[49] No universally agreeable rCBV threshold exists to differentiate HGN from LGN , with Ji Hoon Shin et al , Nail Bulakbasi et al, Meng Law et al and Riyadh N et al suggesting rCBV cut-off values of 2.93, 2.60, 1.75 and 1.75, respectively.[50-53] Gliomas with high rCBV, specifically more than 1.75 progress faster and are associated with a poor prognosis.[52] Friso W. A observed sensitivity and specificity of 70% and 1000% respectively for the rCBVmax cut-off values of 1.85.[15] Due to extravascular leakage of contrast and differences in post-processing software used, the measured rCBV value may not be generalised to all studies.[54] The combination of preload and post-processing correction can significantly improve the accuracy of rCBV values compared to preload.[54] The glioblastoma can be differentiated from PCNSL using corrected CBV (CBV with contrast leakage correction) more accurately than using conventional (uncorrected) CBV parameter.[55] Despite good correlation between rCBV and histological grading, a multi parametric approach combining ADC, rCBV and MRS metabolites ratio contributed to a more accurate diagnosis, compared to these modalities used alone.[53,56,57]

The most DCE studies show increasing K trans and Ve values with progressive tumor grade. However the K trans , Ve and Vp cut-off values differ markedly among studies ,emphasizing the need to consider various confounding factors (type of pharmacokinetic model, contrast agent and T10 among others) while comparing the results among two studies.

Takashi et al found cutoff value of K-trans = 0.0848 and Ve =0.18 provided the best good combination of sensitivity and specificity for diagnosis of LGG.[36] These values of

k-trans and Ve yield sensitivity and specificity (0.88 and 1.0) and (0.96 and 1.0) respectively.

Corrado Santarosa et al observed sensitivity and specificity of 100% and 90% respectively for the rCBV max cut-off values of 1.85. In this study the authors also documented sensitivity and specificity of 100% for both the Vp (max) cut-off value of 2.25 mL/100 and K trans (max) cut-off value of 0.019.[12]

Li et al found cutoff value of K-trans = 0.054 and Ve =0.296 provided the best good combination of sensitivity and specificity for differentiation for LGG from HGG. These values of k-trans and Ve yield sensitivity and specificity (94.1% and 93.3%) and (92.9% and 91.7%) respectively.[58]

Kickingereder et al in their study comprising 11 PCNSL and 60 GB observed significantly higher median volume transfer constant (K-trans) and flux rate constant (Kep) values (0.145 ± 0.057 and 0.396 ± 0.088) in PCNSL than in GB (0.064 ± 0.021 and 0.230 ± 0.058). ROC analysis showed k-trans cut-off value of 0.093 had the best discriminative value to discriminate the two conditions (sensitivity, 90.9%; specificity, 95.0%).Similarly, Ve values also showed higher trend in PCNSL (0.434 ± 0.165) than glioblastoma (0.319 ± 0.107) , but did not reach significance.[59]

Do Vp , k-trans and rCBV hotspots co-localise ?

Corrado Santarosa in their study comprising 26 treatment naïve glioma patients who underwent 3T-MR DCE and DSC imaging (using a gadolinium contrast dose, splitted in two boluses) demonstrated equal accurateness of Vp and rCBV for glioma grading and emphasized that these two parameters depict the neoangiogenesis. Also, K-trans hotspots co-localized with Vp hotspots only in 56% of the enhancing glioma regions, supporting the view that these two parameters though equally useful in glioma grading

depict different physiological information. The Combination of Vp and K-trans parameters improved the overall diagnostic performance in glioma grading.[12]

Similarly , P. Alcaide-Leon, in their study comprising 32 HPE proven Glioblastoma found very weak correlation following voxel-by -voxel comparison of k-trans , Vp and CBV , suggesting different physiological information provide by these parametric maps. Also, they attributed the findings of significantly higher blood volume obtained by DCE MR compared to DSC MR imaging to the effect of contrast leakage.

Moran Artzi et al in their study evaluating vp and CBV values in both the healthy subjects and glioblastoma found high correlations between the both parameters in healthy as well as glioblastoma patients and therefore proposed DCE as an alternative method to DSC for blood volume assessment, considering the advantages of higher spatial resolution , less susceptibility artifacts, as well as additional information of tissue permeability provided by the former method.[18]

The findings of high rCBV values in oligodendrogliomas (irrespective of glioma grade) is attributed also to its predominant cortical location(and therefore prominent susceptibility variations from adjacent cortical macro-vessels and venous vessel) and not merely to its unique “chickenwire” microvessel network pattern. The DCE - MRI overcome these vessels induced susceptibility effects and therefore has the potential to reduce the rCBV values overlap between low-grade and high-grade oligodendrogliomas.[60]

Lymphoma versus GBM:

The marked difference in the management strategy between the PCNSL and GBM makes the preoperative differentiation of the two highly relevant.[61]

Similarly, Permeability indices, including K-trans, have been shown in number of earlier studies to correlate with glioma grade but to overlap with Lymphoma.[17,62] Due to the difference in the degree of neovascularization between the PCNSL and GBM, most of the studies show significantly lower rCBV values in the former compared to the latter.[48,63]

However, Kickingereder et al observed significantly higher k-trans and kep values in PCNSL compared to GBM (but no difference in Ve values)and also noted sensitivity of 90.9% and specificity of 95.0% using the k-trans cut-off value of 0.093. The higher k-trans and kep values in PCNSL (compared to GBM) may be attributed to less flow limited behavior to the contrast agent uptake in the former.[59]

Toh et al compared DSC MR derived pseudoleakage parameter K2 (following mathematic leakage-correction model) in PCNSL and GB and observed significantly higher values in the former.[55,64,65] However Kickingereder et al noted superior diagnostic performance of DCE-derived K-trans compared to DSC-derived K2.[59] Also, more closer relationship between K2 and K-trans was specifically observed at high flip angles **.** The clinical utility of K2 and further correlation with K-trans remains to be determined in future studies.[64]

The DCE MR perfusion parameters show overlapping values between high grade glioma, metastases and lymphoma, while the later fairly consistently shows lower CBV on DSC MR . Ve in lymphoma is documented to be higher than of HGG and so could help differentiate the two conditions.[36]

A few features which help in differencing GBM and PCNSL using MR perfusion are summarized in Table 3.

Parameters	Lymphoma	GBM
Rx	biopsy-only	maximal safe resection
Uptake of contrast in tumor	less flow-limited	More flow-limited
K-trans & Kep	Lymphoma>GBM	Less than with lymphoma
K2	Lymphoma>GBM	less than with lymphoma
rCBV (uncorrected)	Relatively lower	Very high (d/t neovasculaity)
rCBV (uncorrected)	May be higher	Very high (d/t neovasculaity)

Table 3

2016 Updates to the WHO Brain Tumor Classification System:

Prior to the 2016 update, the WHO CNS classification was solely based on factors which could be evaluated at histopathology. Although knowledge related to molecular and genetic role in brain tumors was available, it has presently been incorporated directly for the first time into the definitions of tumors rather than its mere descriptive usage.[66]

Layered Diagnosis

Under the new WHO classification schema, molecular and genetic data supplements the histologic classification with intertwined categories of information, a concept of the layered diagnosis for CNS tumors.[66] Layer 1 depicts the integrated diagnosis, a summation of the molecular and morphologic data into the single diagnostic entity that best describes the tumor (Table 4).

Layer 1	The final integrated diagnosis
Layer 2	Histological classification
Layer 3	WHO grade
Layer 4	Molecular classification

Table 4 : Layered diagnosis of CNS tumors. The Integrated diagnosis (layer 1) comes last, following the definition of layers 2–4 .

The IDH mutation has become definitional for infiltrating gliomas in adults, with 1p/19q codeletion further characterizing the type. The 1p/19q codeletion being a diagnostic criteria for oligodendroglioma and characteristically absent in astrocytoma (Fig 2).

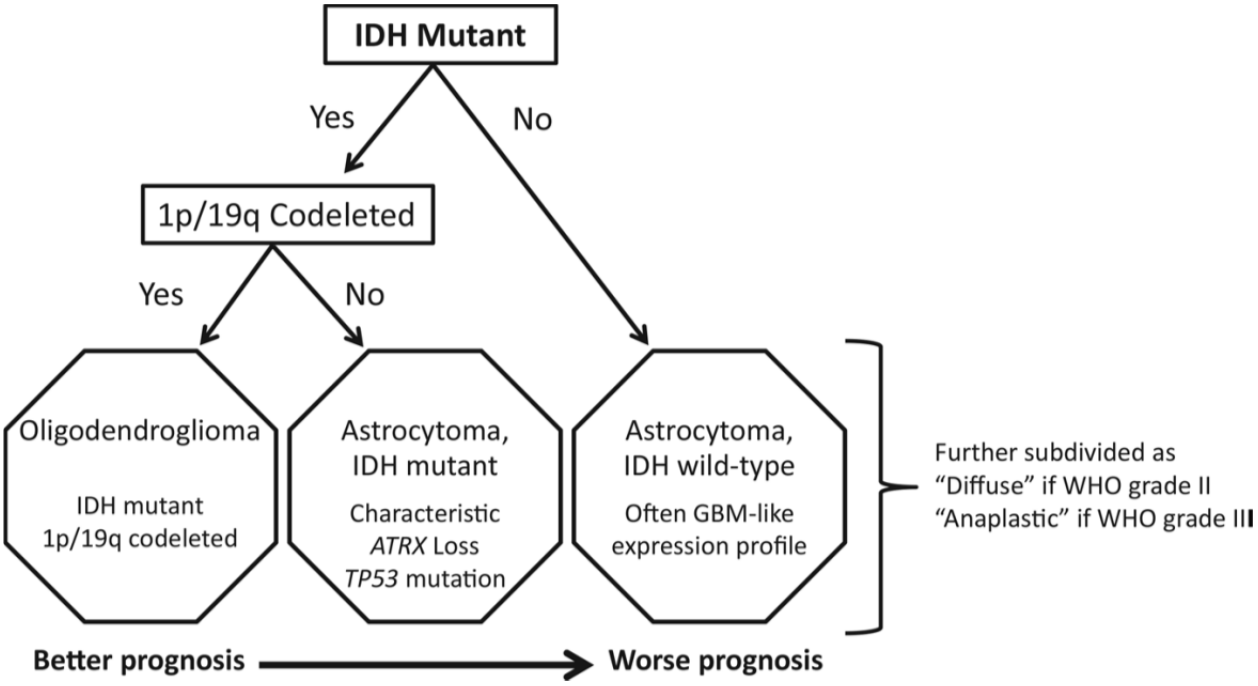

Fig 2

Table 5 depicts the Imaging Features of 1p19q Codeleted versus Intact Oligodendrogliomas.[67] The Table 6 demonstrates distinctive Imaging Features of 1p19q Codeletion, IDH Mutation, and MGMT Promotor Methylation tumors. [67] The table 7

shows conventional and advanced imaging features of MGMT Promotor Methylated versus Unmethylated High-Grade Glioma**.** [67]

Feature	**1p19q Codeletion**	**1p19q Intact**
Localization	Frontal, parietal, and occipital predominance	Temporal, insular, and temporoinsular predominance
Calcifications	Common (40%)	Uncommon (20%)
Signal intensity	Heterogeneous	Homogeneous
ADC	No difference–lower maximum ADC	No difference
rCBV	Mildly elevated in grade II	Not elevated in grade II
Fluorodeoxyglucose	Mildly increased uptake	Not increased

Table 5

1p19q Codeletion	**IDH Mutation**	**MGMT Promoter Methylation**
T2-weighted heterogeneity, especially when assessed with texture analysis	Presence of 2-HG on MRS	Increased k-trans
Calcifications	Frontal lobe	-
Mildly elevated rCBV	Large unenhancing portion	-
Increased fluorodeoxyglucose uptake	Sharp border	-

Table 6

Feature	MGMT Methylated	MGMT Unmethylated
Localization	Possibly left hemisphere: temporal, parietal, or occipital lobe	Right hemisphere: temporal lobe, basal ganglia, subventricular zone
Enhancement	Not different, mixed nodular	Not different, ring
Edema	less edema associated with better prognosis	extensive; no correlation with prognosis
ADC	Lower	Higher
rCBV	Not different, lower	Not different, higher
K-trans	Increased	Decreased

Table 7

Major Changes in 2016 CNS WHO classifications (compared to 2007 classification):

- Major restructuring of diffuse gliomas, with incorporation of genetically defined entities
- Major restructuring of medulloblastomas, with incorporation of genetically defined entities
- Major restructuring of other embryonal tumors, with incorporation of genetically defined entities and removal of the term "primitive neuroectodermal tumor"
- Incorporation of a genetically defined ependymoma variant
- Some tumors are defined by a combination of microscopic morphologic and molecular and genetic factors, whereas others continue to be defined by morphology alone.
- SFT and HPC have been combined under the common name SFT/HPC, which can be classified as WHO grade I, II, or III.

Addition of newly recognized entities, variants and patterns

- Glioblastoma, IDH-wildtype and Glioblastoma, IDH-mutant (entities)
- Diffuse midline glioma, H3 K27M–mutant (entity)
- Embryonal tumor with multilayered rosettes, C19MC-altered (entity)
- Ependymoma, RELA fusion–positive (entity)
- Diffuse leptomeningeal glioneuronal tumor (entity)
- Anaplastic PXA (entity)
- Epithelioid glioblastoma (variant)
- Glioblastoma with primitive neuronal component (pattern)
- Multinodular and vacuolated pattern of ganglion cell tumor (pattern)

Deletion of former entities and variants

Gliomatosis cerebri
Protoplasmic and fibrillary astrocytoma variants
Cellular ependymoma variant

Diffuse Midline Glioma, Histone H3 K27M-Mutant

Before the new 2016 classification, the pediatric brainstem infiltrating glioma was conventionally referred to as diffuse intrinsic pontine glioma (DIPG). The Recent investigations into the underlying genetic makeup of these lesions show that approx. 60%–80% of these harbor mutations at position K27 in the gene for histone H3 as opposed to 14%– 22% of non–brainstem gliomas with this mutation**.** [68-70] The DMG are categorized as grade IV tumors (regardless of histological features) and although most commonly involve pons and thalami, the involvement of cerebellum, spinal cord, and other midline structures, including the hypothalamus, third ventricle and pineal region is also involved rarely**.** [69,71]

These tumors are predominantly noted in children or young adult with average age of presentation being 24 years in thalamus epicentred , 7 years in pontine and 28 year in spinal cord lesions**.** [69] DMG with H3 K27M-mutant demonstrate variable imaging features, with thalamic , pontine and cervical spine lesions showing 50%, 67% and 100% enhancement respectively**.** [68]

Materials and Methods

MATERIALS AND METHODS

Institutional Ethics Committee (IEC) approval was obtained vide letter No. **SCT/IEC/940/AUGUST-2016.** This was a prospective study conducted in department of IS&IR, SCTIMST, between August 2016 and 30 June 2018.

Subjects

This prospective study was approved by the ethical committees of our Institution and prior written informed consent obtained from all patients.

Adult (> 18 years) patients who were referred to our Institution with suspected gliomas of varying grades and underwent MRI with the predetermined protocol at our institute (including conventional sequences , DCE and DSC MR perfusion) were enrolled in the study. Exclusion criteria included patients < 18 years, allergy to gadolinium-based contrast agent, extraxial brain masses, prior steroid , surgery, radiation or chemotherapy. Following MR imaging, patients underwent surgery either as tumor resection or biopsy. The histologic examination and grade determination was performed according to the 2016 WHO criteria.

Based on the inclusion criteria, a total of 52 patients were finally included in this study for statistical analysis.

Imaging protocol

Examinations were performed on a 3 T MR scanner (Discovery 750, GE Healthcare, Milwaukee, WI) using a standard 24 channel head coil. Pre-contrast T1- weighted, T2-weighted ,T2- FLAIR , diffusion-weighted and SWI images were acquired.

A cumulative dose of 0.1 mmol/kg body weight of gadobutrol (Gadovist, 1 mmol/mL; Bayer Schering Pharma, Berlin, Germany) was administered, splitted in two equal boluses. The first bolus was injected after the start of the DCE sequence by using a

power injector (Spectris Solaris MR injector; MedRad, Indianola, Penn-sylvania) at a rate of 3 mL/s, immediately followed by a 20 mL continuous saline flush at the same injection rate. The second bolus was injected following the third dynamic acquisition of the DSC sequence by using the same power injector at a rate of 5 mL/s, followed by a 20 mL saline flush at the same injection rate. An interval of 6 minutes was maintained between the two injection administration. Therefore, the contrast administration during DCE pre-saturated the tissue for the DSC-MR sequence. After completion of the DSC MR imaging sequence, standard postcontrast 3D BRAVO data and MR spectroscopy were acquired. DCE-MRI was acquired using a 3D fast spoiled gradient echo sequence . The MR parameters employed for DCE and dsc perfusion are summarized in table 1.

Parameters	**DCE MR Perfusion**	**DSC MR Perfusion**
TR/TE (msec)	4.3/0.8	2000/30
Slice thickness (mm)	5	5
Flip angle (degree)	25	60
Matrix	128 x 128	96 x 96
Measurements	50	42
Temporal spacing (sec)	6.48	2
Time duration (sec)	324	84

All imaging data were then transferred from scanner to a workstation (Advantage Workstation 4.6, GE Medical Systems, Milwaukee, WI). The DCE data was analyzed using Tofts model implemented in the commercially available GenIQ (GE Medical Systems, Milwaukee,

WI) software. The 3-D, rigid motion correction (employs a combination of rotational and translation movement) was employed in all patients. The software automatically

extracted the pixels that it considered to be arteries or veins based on the temporal changes in signal intensity of the voxels. Fixed T1 method and default T10 value (T10 = 1000 ms) were used in the analysis.

The Regions of interest were defined by the radiologist on axial postcontrast and FLAIR datasets, specifically avoiding the cystic, necrotic and hemorrhagic areas. For each tumor, 5 to 10 ROIs were manually positioned on the corresponding slices of Ktrans and Ve maps .On each parametric map, the hotspot (region of maximal abnormality) within the lesion volume was determined with visual inspection and selections of ROIs continued unless a maximal quantitative value inside an ROI was acquired.

The CBV maps were calculated following application of tracer kinetic model to the first-pass data. The contrast bolus administered during the DCE acquisition also compensated for the T1 contamination of the DSC sequences. The rCBV was obtained by dividing the maximum CBV value in the tumor volume to the CBV value of an ROI positioned in the contralateral normal-appearing white matter.

Statistical analysis

Analysis and statistical figures were calculated using SPSS version 22.0

For all statistical tests, $P < 0.05$ was considered statistically significant.

Quantitative Variables were expressed as mean, standard deviation median and inter quartile range. Qualitative variable were expressed as frequency and percentage. Comparison of quantitative variables between two groups were analysed by independent sample t test. Receiver operating characteristic (ROC) curve analysis was used to evaluate performance of k-trans, Ve and rCBV in discriminating HGG from LGG, WHO grade II from III , grade III from grade IV and grade II from IV glioma by

comparing the areas under the curve (AUC). The optimum cut off Value , Sensitivity and specificity were calculated accordingly to differentiate these grades.

HPE ;

An experienced neuropathologist provided histopathologic diagnosis according to the World Health Organization (WHO) 2016 classification.

Immunohistochemistry:

Immunostains for R132H-mutant IDH1 and K27M-mutant H3.3 were scored as positive or negative, ATRX as intact or loss of nuclear expression. Fluorescence In Situ Hybridization (FISH) for 1p/19q co-deletion were not performed in any of the tumors.

Microvessel Density assessment:

Immunohistochemistry (IHC) for CD31 was performed in total of 39 case of high grade glioma, comprising 13 GB (13/13), 16 AA (16/16), 7 AODG (7/8) and 3 DMG (3/4) cases. In one case each of AODG and DMG, the IHC could not be performed due to non-availability of paraffin blocks / insufficient tissue being present. Also, the MVD was not calculated for low grade glioma , considering the limited number of HPE proven low grade glioma in our study.

The CD31 immunostained sections were photographed using Leica DFC450 C digital microscope camera (Leica Microsystems, Wetzlar, Germany). The microvessel density was calculated based on modification of the method described by Cai H et al**.** [72] Ten fields with highest number of blood vessels were photographed using 25X objective. The microvessel density (MVD) per mm^2 was calculated as the average of five fields with the highest MVD.

RESULTS

RESULTS

A total of 52 patients with intraxial brain masses fulfilling the inclusion criteria were included and evaluated in the study. Among the cases included in our study, 30 were male and the rest (22 /52) were female (Table 1).

Sex	Number of patients (n)	Percent (%)
Male	30	57.7
Female	22	42.3
Total	52	100.0

Table 1: Sex wise distribution of the cases

46 of the total 52 patients underwent HPE evaluation and were classified according to 2016 WHO Classification of Tumors of the Central Nervous System.

The 6 of the 8 cases of low grade glioma included in the study did not undergo HPE and were assumed to be grade 2 based on the stable low values of k-trans, Ve , Kep and rCBV over 2 years.

The HPE evaluated cases comprised two WHO grade II (2/46, 4.3%), 24 WHO grade III (52.1%), 17 WHO grade IV tumors (36.9%) and 3 cases of PCNSL (6.5%). The WHO grade IV tumors included: glioblastoma (13/17, 76.4%) and diffuse midline glioma H3 K27M mutant (4/17, 23.5%). Of the 13 Glioblastoma cases, IDH-wildtype comprised 11 (11/13, 84.6%) and the IDH-mutant type comprised 2 (2/13, 15.3%) .

The WHO grade III tumors included 9 cases of IDH-mutant anaplastic astrocytoma (9/24, 37.5%), 7 cases of anaplastic astrocytoma NOS (7/24, 29.1%) and 8 cases of anaplastic oligodendroglioma NOS (8/24, 33.3%).

The both cases of HPE proven WHO grade II tumor were IDH-mutant diffuse astrocytoma.

The HPE was done on the excised sample in all cases of AODG, and one but all cases of AA and GB. All DMG and one but all cases of PCNSL underwent HPE evaluation following biopsy. The mode of obtaining tissue sample is depicted in Table 2.

Excision or Biopsy	HPE				
	AA	AODG	GB	PCNSL	DMG
Biopsy	1	0	1	2	4
Excision	15	8	12	1	0
Total	16	8	13	3	4

Table 2: Mode of obtaining tissue sample

The HPE and/or age wise distribution of the cases is depicted in Table 3, 4 and 5 and figure 1. The lobar / side wise distribution and the IDH status of the various tumors is listed in tables 6 and 7 respectively.

Diagnosis	Frequency	Percent
LGG	8	15.4
AA	16	30.8
AODG	8	15.4
GBM	13	25.0
PCNSL	3	5.8
DMG	4	7.7
Total	52	100.0

Table 3 : Percentage distribution of different intraxial masses. GB : Glioblastoma , AA : Anaplastic astrocytoma, AODG : Anaplstic oligodendroglioma , LGG : low grade Glioma, DMG: diffuse midline glioma , PCNSL: Primary CNS Lymphoma

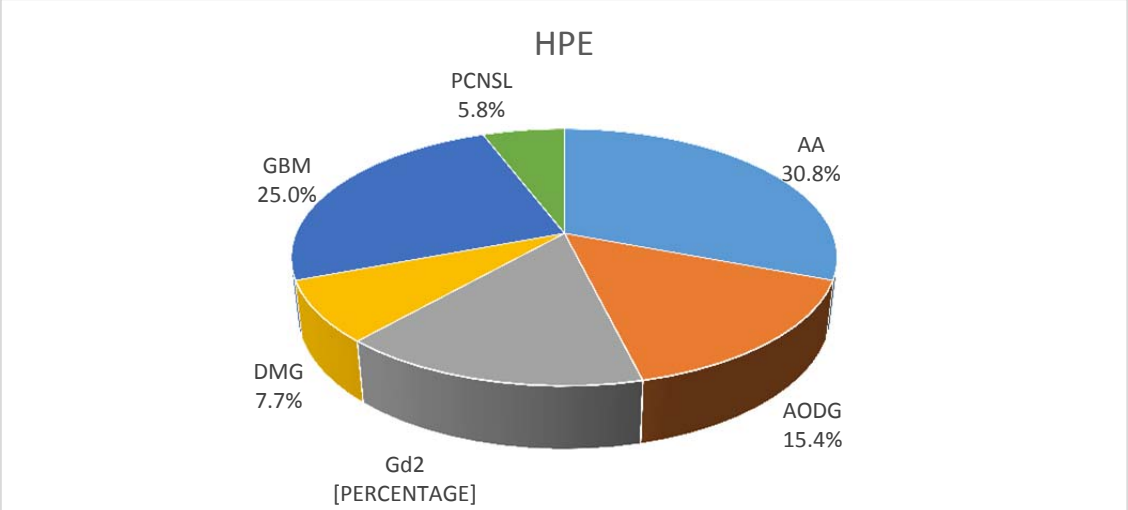

Fig 1: Percentage distribution of different intraxial masses.

	HPE								Total	
	Gd II		AA (Gd III)		AODG(Gd III)		GB(Gd IV)			
Sex	n	%	n	%	n	%	n	%	n	%
Male	2	25	9	56.3	4	50	10	76.9	25	55.6
Female	6	75	7	43.8	4	50	3	23.1	20	44.4
Total	8	100	16	100	8	100	13	100	45	100

Table 4: Sex and HPE tumor grade based distribution of cases.

Age Gp (Years)	<20	21-30	31-40	41-50	51-60	61-70	71-80
GB	-	1	1	3	2	5	1
AA	-	4	3	7	2	-	-
AODG	-	-	3	3	2	-	-
LGG	-	-	4	4	-	-	-
DMG	-	-	-	1	2	-	-
PCNSL	1	2	1	-	-	-	-

Table 5: Age and HPE based distribution of different intraxial masses.

Pathology	Frontal R L	Temporal R L	Parietal R L	Occipital R L	BG R L	Thalamus R L
GB	3 2	1 4	2 1	- -	-	- -
AA	7 5	1 2				
AODG	4 2	1 1				
LGG	2 3	1 1	1			
DMG						4
PCNSL	1				1	1

Table 6 : Side and affected lobe/structure wise distribution of various lesions

IDH	AA	AODG	GB	DMG
M	8	8	2	0
W	7	0	11	0
ND	1	0	0	4
Total	16	8	13	4

Table 7: IDH status based distribution of various intraxial tumors

Low grade Glioma (LGG): The average k-trans value noted was 0.052(varied from 0.032 to 0.072). The average Ve value was 0.020, and varied from 0.012 to 0.037. The average rCBV value noted was 1.03 (varied from 0.70 to 1.28).

Glioblastoma (GB): The average k-trans value was 0.280, and varied from 0.080 to 1.176. Average Ve value was 0.351 (varied from 0.137 to 1.000). The average rCBV value noted was 6.090 (varied from 2.73 to 12.09).

Diffuse midline Glioma (DMG) : The average k-trans value noted was 0.285, and varied from 0.080 to 0.446 Average Ve value was 0.291 (varied from 0.046 to 0.454). The average rCBV value was 6.37, and varied from 3.93 to 12.34.

Anaplastic Astrocytoma (AA): The average k-trans value was 0.248, and varied from 0.034 to 0.688. Average Ve was 0.135 (varied from 0.009 to 1.000). The average rCBV value was 3.23, and varied from 0.58 to 7.86.

Anaplastic Oligodendroglioma (AODG): The average k-trans value noted was 0.165 (varied from 0.033 to 0.464). Average Ve value was 0.077 and varied from 0.008 to 0.352. The average rCBV value was 4.13 (varied from 1.21 to 10.79).

Primary central nervous system lymphoma (PCNSL): The average k-trans value noted was 0.204, and varied from 0.137 to 0.252. The average Ve value noted was 0.516 (varied from 0.266 to 0.821).The average rCBV value noted for PCNSL was 5.84, and varied from 1.04 to 10.32.

Diagnosis	**N**	**K-trans**						
		Mean	**SD**	**Min**	**Max**	**Median**	**Q1**	**Q3**
LGG	8	0.05	0.02	0.032	0.080	0.048	0.036	0.068
AA	16	0.25	0.22	0.034	0.688	0.156	0.055	0.465
AODG	8	0.17	0.14	0.033	0.464	0.128	0.050	0.245
GB	13	0.28	0.30	0.048	1.176	0.204	0.104	0.305
PCNSL	3	0.20	0.06	0.137	0.252	0.224	0.137	0.000
DMG	4	0.29	0.16	0.080	0.446	0.308	0.126	0.423

Table 8 : K-trans values among various brain tumors. Interquartile range. Q1 denotes 25th percentile and Q3 the 75th percentile.

Diagnosis	N	Ve						
		Mean	SD	Min	Max	Median	Q1	Q3
LGG	8	0.02	0.01	0.012	0.037	0.018	0.013	0.025
AA	16	0.13	0.24	0.007	1.000	0.062	0.026	0.150
AODG	8	0.08	0.11	0.008	0.352	0.038	0.022	0.078
GB	13	0.33	0.23	0.137	1.000	0.249	0.192	0.421
PCNSL	3	0.52	0.28	0.266	0.821	0.463	0.266	0.000
DMG	4	0.29	0.19	0.046	0.454	0.334	0.092	0.450

Table 9 : Ve values among various brain tumors. Interquartile range. Q1 denotes 25th percentile and Q3 the 75th percentile.

Grade	N	rCBV						
		Mean	SD	Min	Max	Median	Q1	Q3
LGG	8	1.04	0.19	0.700	1.280	1.030	0.918	1.220
AA	16	3.24	2.25	0.580	7.860	2.705	1.233	4.773
AODG	8	4.13	3.43	1.210	10.790	3.105	1.375	6.520
GB	13	6.09	2.88	2.730	12.090	5.190	3.900	8.095
PCNSL	3	5.85	4.65	1.040	10.320	6.190	1.040	0.000
DMG	4	6.37	4.01	3.930	12.340	4.605	3.990	10.515

Table 10: rCBV values among various brain tumors. Interquartile range. Q1 denotes 25th percentile and Q3 the 75th percentile.

The scatter plot diagram depicts the distribution of K-trans, Ve and rCBV values according to different intraxial masses In Fig 2, 3 and 4 respectively.

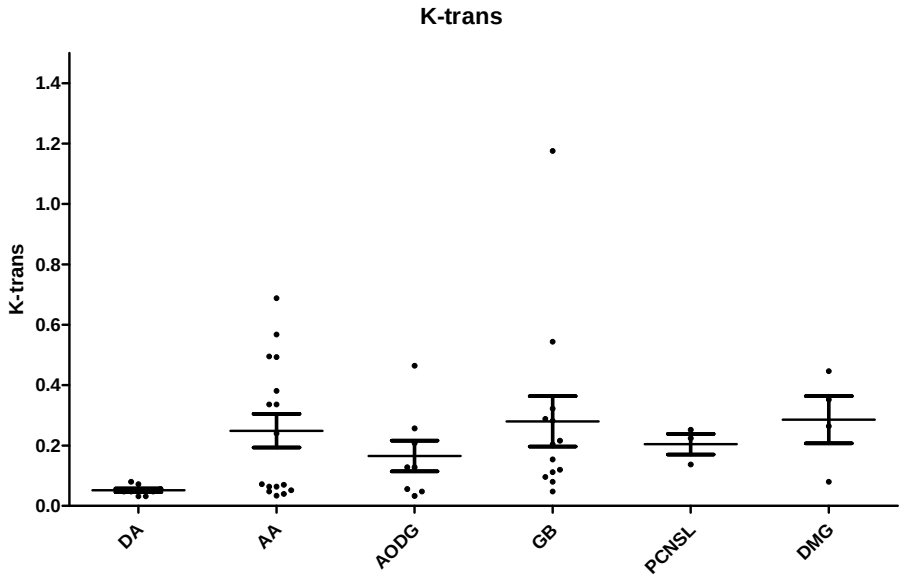

Fig 2 : Scatter plot diagram depicts distribution of K- trans values in different intraxial masses

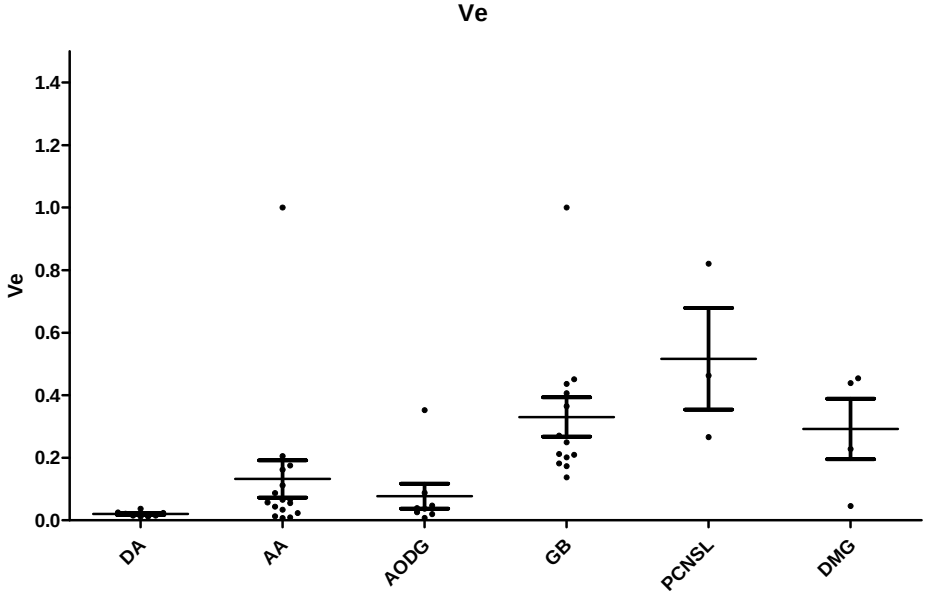

Fig 3: Scatter plot diagram depicts distribution of Ve values in different intraxial masses

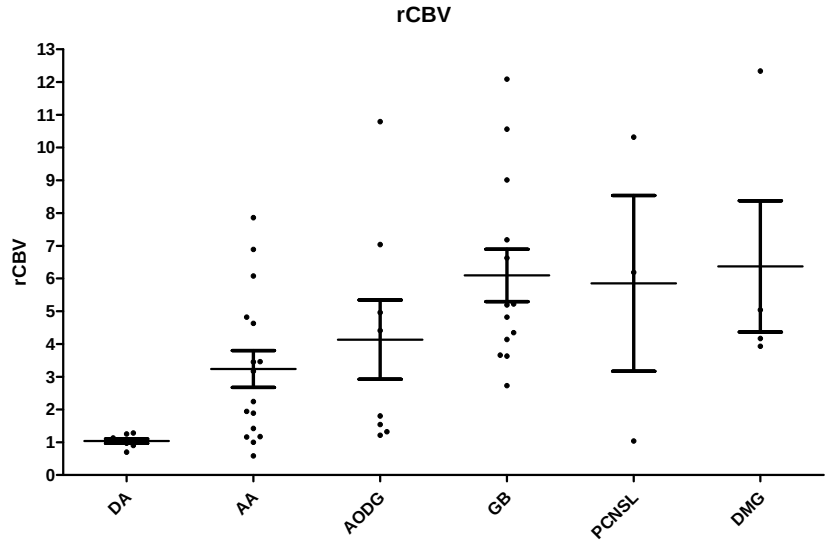

Fig 4: Scatter plot diagram depicts distribution of rCBV values in different intraxial masses

LGG versus HGG: The DCE perfusion parameters (k-trans and Ve) as well as DSC perfusion parameter (rCBV) showed statistically significant differences in parametric values in differentiating the LGG and HGG. Although k-trans , Ve and rCBV all reached statistical significance, the later achieved the maximum statistical significance (Table 11).

Within the independent parametric variables, the area was highest for rCBV (0.938), though similar high values were seen for K-trans and Ve (0.848 and 0.867 respectively).

	N	K-trans		t	p
		Mean	SD		
Low grade	8	0.052	0.017	2.232	0.031
High grade	37	0.242	0.238		
	N	Ve		t	p
		Mean	SD		
Low grade	8	0.020	0.009	2.028	0.049
High grade	37	0.190	0.235		
	N	rCBV		t	p
		Mean	SD		
Low grade	8	1.036	0.190	3.209	0.003
High grade	37	4.434	2.966		

Table 11: The DCE (K-trans and Ve) and DSC (rCBV) perfusion parameters effectiveness in differentiating LGG and HGG

MVD assessment:

Immunohistochemistry (IHC) with CD31 was performed in total of 39 cases of high grade glioma, comprising 13 GB (13/13), 16 AA (16/16), 7 AODG (7/8) and 3 DMG (3/4). In one case each of AODG and DMG, the IHC could not be performed either due to non-availability of paraffin blocks or/and insufficient tissue being present. Also, the MVD was not calculated for low grade glioma , considering the limited number of HPE proven low grade glioma in our study.

The microvessel density (MVD) in WHO grade III tumors ranged from 42.3-245.2/mm^2 with mean MVD of 114.7/mm^2 (standard deviation, SD = 7.2). In WHO grade IV tumors it ranged from 37.3-304.2/mm^2 with mean MVD of 141.5/mm^2 (SD = 10.6). The average MVD in different histological subtypes were: 104.8/mm^2 in glioblastoma IDH-wildtype, 181.6/mm^2 in glioblastoma IDH-mutant, 79.1/mm^2 in diffuse midline glioma (H3 K27M-mutant), 110.5/mm^2 in anaplastic astrocytoma IDH-mutant, 104.2/mm^2 in anaplastic

astrocytoma NOS and 129.3/mm^2 in anaplastic oligodendroglioma NOS. Table 12 and 13 shows the distribution of MVD values in different intraxial tumors.

Diagnosis	N	MVD						
		Mean	SD	Min	Max	Median	Q1	Q3
AA	16	110.78	55.09	42.26	221.13	100.99	69.78	143.12
AODG	7	128.75	62.73	49.63	245.21	117.44	95.82	168.55
GB	13	139.86	73.89	45.21	304.17	127.76	85.52	185.51
DMG	3	79.11	58.47	37.35	145.94	54.05	37.35	0.00

Table 12: MVD values in different intraxial tumors.

Grade	N	MVD						
		Mean	SD	Min	Max	Median	Q1	Q3
AA+ AODG	23	116.2	56.7	42.3	245.2	108.6	74.2	149.9
GB	13	139.9	73.9	45.2	304.2	127.8	85.5	185.5
DMG	3	79.1	58.5	37.4	145.9	54.1	37.4	0.0

Table 13: MVD values in different intraxial tumors. AA+ AODG : combined grade 3 tumors.

The Pearson correlation coefficient between MCD and k-trans , MCD and Ve and between MCD and rCBV was 0.445, 0.017 and 0.522 respectively (Table 14) . Scatter plot shows correlation between MVD and the MR perfusion parameters (K-trans, Ve and rCBV) and is depicted in Fig 5, 6 and 7. The Pearson correlation coefficient shows strongest positive correlation with rCBV and weakest with Ve.

Correlation of MVD with other parameters	K-trans	Ve	rCBV
Pearson Correlation r	.445	.017	.522
p	.004	.919	.001
N	40	40	40

Table 14 : Correlation of MVD with k-trans, Ve and rCBV.

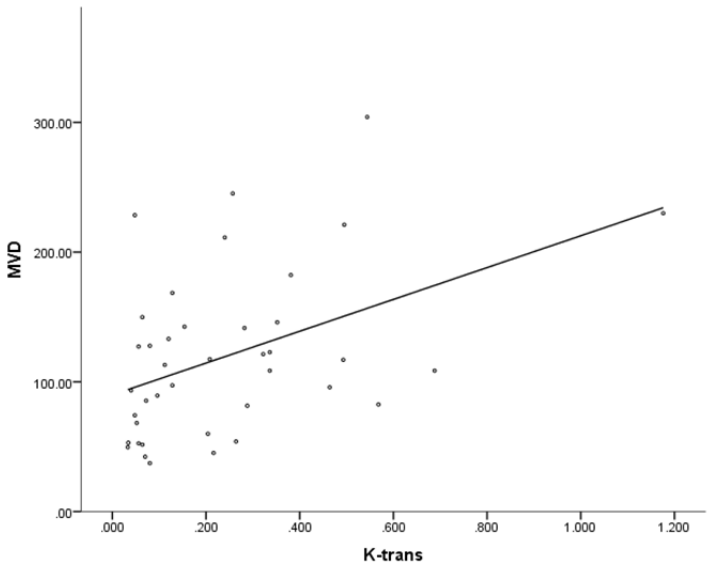

Fig 5 : Scatter plot showing correlation between MVD and K-trans

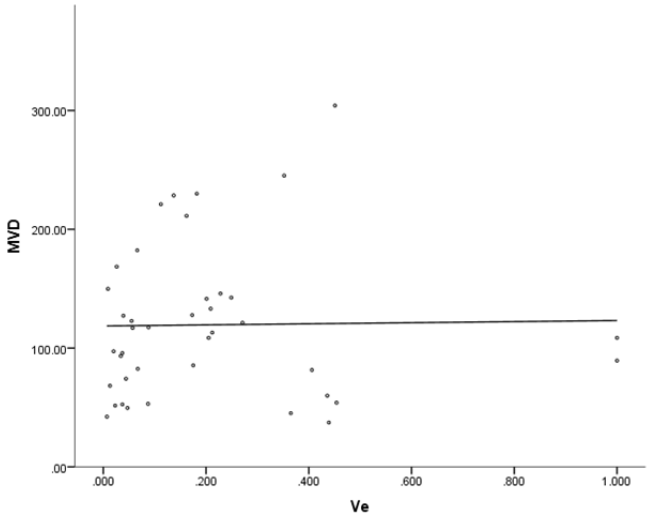

Fig 6 : Scatter plot showing correlation between MVD and Ve

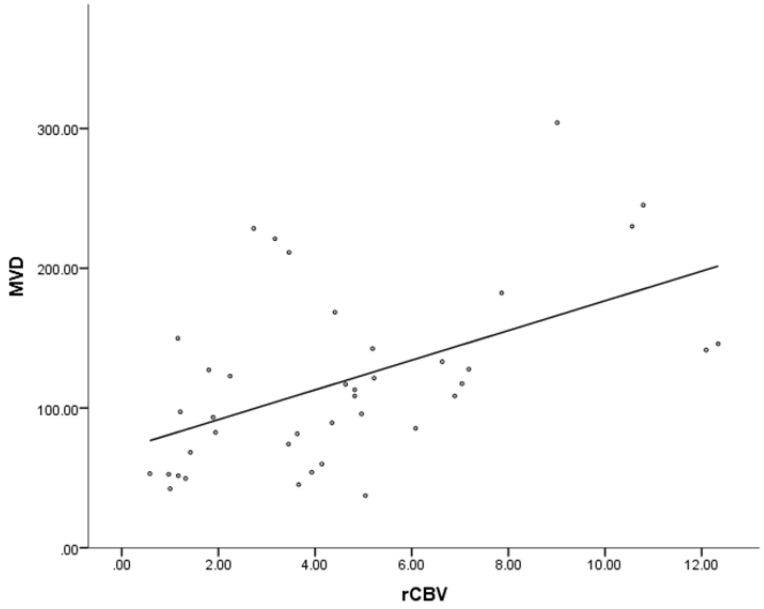

Fig 7: Scatter plot showing correlation between MVD and rCBV

High grade versus low grade: ROC curve (K trans, Ve and rCBV)

Within the independent parametric variables, the AUC was highest for rCBV (0.938), with similar high AUC noted for K-trans and Ve (0.848 and 0.867 respectively) (Table 15 and Fig 8).

	AUC	**SE [a]**	**95% CI [b]**
K-trans	0.848	0.0606	0.710 to 0.937
Ve	0.867	0.0531	0.732 to 0.949
rCBV	0.938	0.0359	0.823 to 0.988

Table 15: Correlation of AUC values of K trans, Ve and rCBV with High grade and low grade glioma differentiation. a= SE : Standard Error , b= 95% CI- 95% confidence interval

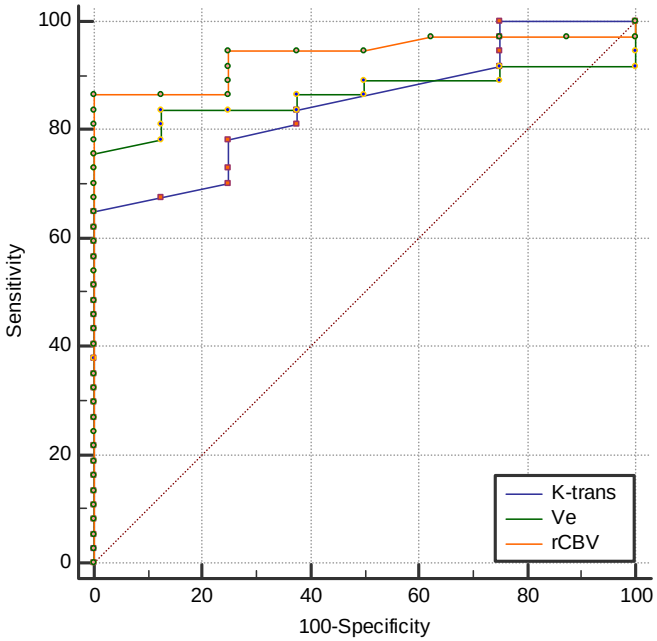

Fig 8 : **High grade versus low grade: ROC curve (K trans, Ve and rCBV)**

K-trans Cut-off value of 0.080 differentiated LGG from HGG with a sensitivity of 64.8 % and specificity of 100%. Also, k-trans Cut-off value of 0.056 differentiated LGG from HGG with a sensitivity of 78.38 % and specificity of 75 %.

Ve Cut-off value of 0.037 differentiated LGG from HGG with a sensitivity of 75.68 % and specificity of 100%. Also, Ve Cut-off value of 0.025 differentiated LGG from HGG with a sensitivity of 83.78 % and specificity of 87.50 %.

rCBV Cut-off value of 1.28 differentiated LGG from HGG with a sensitivity of 86.49 % and specificity of 100%. Also, rCBV Cut-off value of 1.13 differentiated LGG from HGG with a sensitivity of 94.59 % and specificity of 75%.

Grade III versus Grade IV : ROC curve (K trans, Ve and rCBV)

Within the independent parametric variables the AUC was highest for Ve (0.912), with AUC noted for rCBV and K-trans as 0.768 and 0.583 respectively) (Table 16 and Fig 9).

	AUC	SE [a]	95% CI [b]
K-trans	0.583	0.0965	0.410 to 0.743
Ve	0.912	0.0498	0.772 to 0.980
rCBV	0.768	0.0771	0.600 to 0.890

Table 16 : Correlation of AUC values of K trans, Ve and rCBV with Grade III versus Grade IV glioma differentiation . SE : Standard Error , 95% CI- 95% confidence interval

k-trans Cut-off value of 0.072 provided the best good combination of sensitivity and specificity (92.31% and 45.83 respectively) for differentiating grade III from grade IV. Ve Cut-off value of 0.112 provided the best good combination of sensitivity and specificity (100% and 79.17% respectively) for differentiating grade III from grade IV. rCBV Cut-off value of 3.46 differentiated grade III from grade IV with a sensitivity of 92.31 % and specificity of 62.50%.

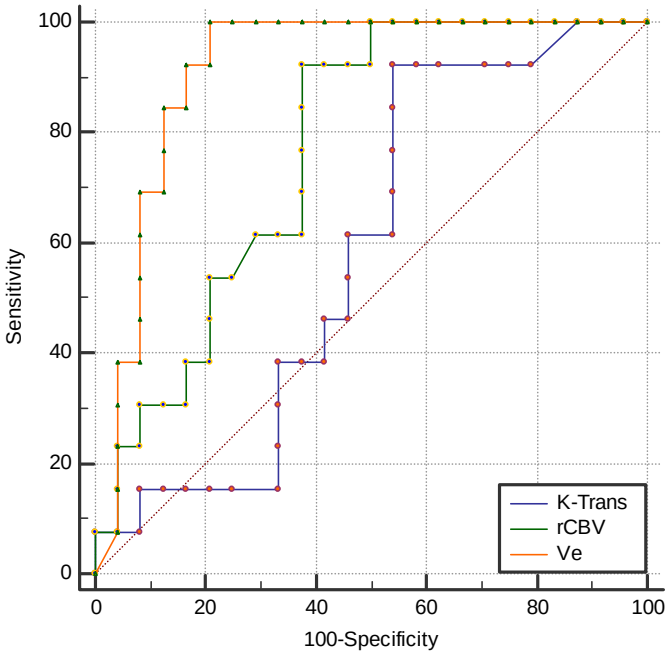

Fig 9 : Grade III versus Grade IV : ROC curve (K trans, Ve and rCBV)

Grade II versus Grade III : ROC curve (K trans, Ve and rCBV)

Within the independent parametric variables the AUC was highest for rCBV (0.904), with AUC noted for K-trans and Ve noted as 0.711 and 0.794 respectively) (Table 17 and Fig 10).

	AUC	**SE [a]**	**95% CI [b]**
K-trans	0.711	0.135	0.524 to 0.857
Ve	0.794	0.0783	0.615 to 0.916
rCBV	0.904	0.0544	0.746 to 0.979

Table 17 : Correlation of AUC values of K trans, Ve and rCBV with Grade II versus Grade III glioma differentiation . SE : Standard Error , 95% CI- 95% confidence interval

k-trans Cut-off value of 0.052 provided the best good combination of sensitivity and specificity (83.33% and 75.0 respectively) for differentiating grade II from grade III glial tumors. Ve Cut-off value of 0.025 differentiated grade II from grade III with a sensitivity of 75 % and specificity of 87.50%. rCBV Cut-off value of 1.28 provided the best good combination of sensitivity and specificity (79.17 % and 100% respectively) for differentiating grade II from grade III glial tumors.

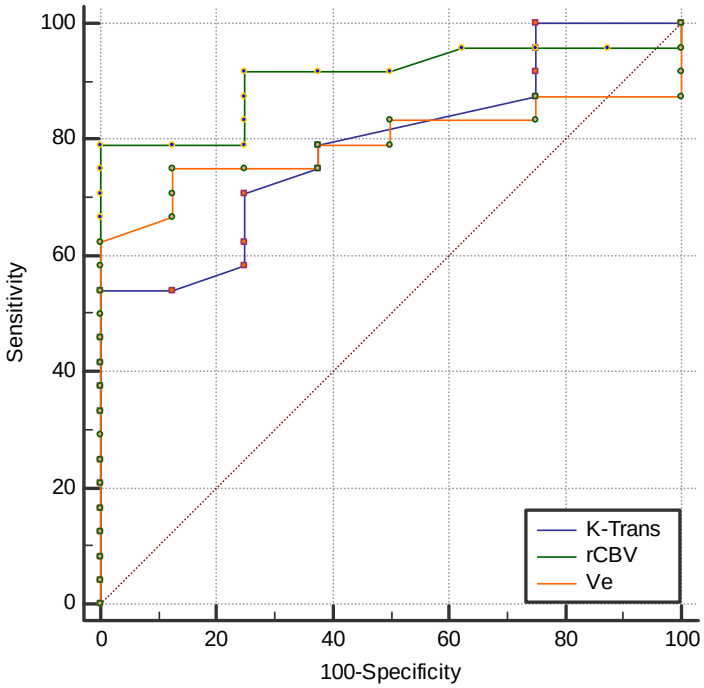

Fig 10 : Grade II versus Grade III : ROC curve (K trans, Ve and rCBV)

Grade II versus Grade IV : ROC curve (K trans, Ve and rCBV)

Within the independent parametric variables the AUC was highest for both rCBV and Ve (1.00 each), with AUC noted for K-trans as 0.952. (Table 18 and Fig 11).

	AUC	**SE [a]**	**95% CI [b]**
K-trans	0.952	0.454	0.761 to 0.999
Ve	1.000	0.0000	0.839 to 1.000
rCBV	1.000	0.0000	0.839 to 1.000

Table 18 : Correlation of AUC values of K trans, Ve and rCBV with Grade II versus Grade IV glioma differentiation . SE : Standard Error , 95% CI- 95% confidence interval

k-trans Cut-off value of 0.080 differentiated grade II from grade III with a sensitivity of 84 % and specificity of 100.0%. Ve Cut-off value of 0.037 provided the best good combination of sensitivity and specificity (100% and 100% respectively) for differentiating grade II from grade III glial tumors .The rCBV Cut-off value of 1.28 differentiated grade II from grade III with a sensitivity of 100 % and specificity of 100%.

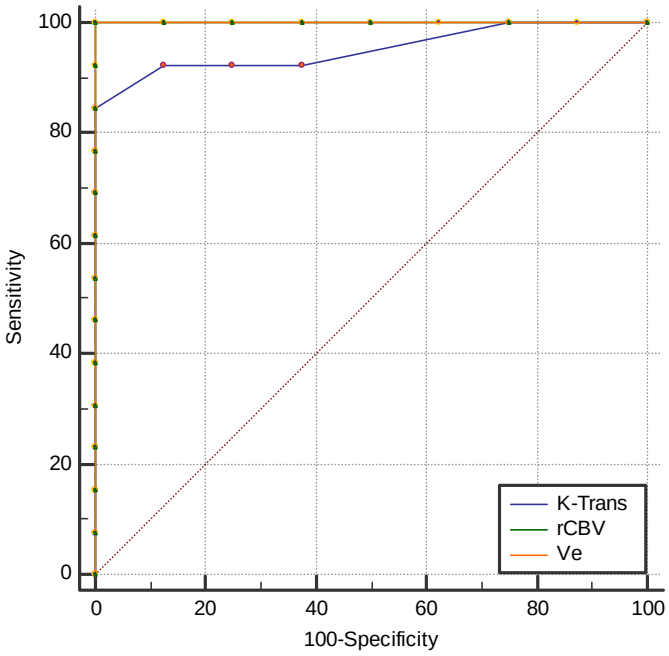

Fig 11 : Grade II versus Grade IV : ROC curve (K trans, Ve and rCBV)

Diffuse midline Glioma (DMG) :

All DMG were evaluated with HPE (biopsy sample) and confirmed following H3 K27M mutant status evaluation. All the four cases were noted centred in the right thalamus , show average age at presentation of 28 years and depict high MR perfusion parameters (k-trans, Ve and rCBV). The average k-trans value noted was 0.285 (varied from 0.080 to 0.446) , Average Ve = 0.291 (varied from 0.046 to 0.454) and the average rCBV = 6.37 (varied from 3.93 to 12.34).

Primary central nervous system lymphoma (PCNSL) :

PCNSL showed mean k-trans = 0.204 (varied from 0.137 to 0.252), Ve = 0.516 (varied from 0.266 to 0.821) and the rCBV = 5.84 (varied from 1.04 to 10.32). Although the Ve values were notably higher in PCNSL, there existed a significant overlap between the PCNSL and GBM. Similarly the k-trans and rCBV showed significant overlap between these two entities.

The higher values of rCBV in our cases can be partly attributed to the preloading of contrast before the DSC scan.

To conclude the results, the mean rCBV , Ktrans, and Ve values were significantly higher in HGGs than those in LGGs ($P < 0.01$). Although the mean rCBV, Ktrans and Ve values of grade IV gliomas showed a trend towards higher values compared to grade III , the statistically significant difference was not achieved. The ROC analysis showed max AUC for rCBV, Ve and rCBV in differentiating LGG from HGG, grade III from IV and grade II from III glioma respectively.

The Pearson correlation coefficient between MVD and k-trans , MVD and Ve and between MVD and rCBV was 0.445, 0.017 and 0.522 respectively with strongest positive correlation noted with rCBV. Trend towards higher MVD values was seen in GBM compared to grade III tumors, however the difference did not reach significance.

All the MR perfusion parameters (k-trans, Ve and rCBV) showed higher values in PCNSL, and there existed a significant overlap in the values between the PCNSL and GBM. Also, All the MR perfusion parameters (k-trans, Ve and rCBV) showed higher values in DMG with a significant overlap with GBM.

Representative Cases

REPRESENTATIVE CASES

CASE 1

41–year- female presented with paresthesia involving right side of the face and right arm.

The MR Imaging (Fig 1) show well circumscribed lesion epicentred in the left insular region.

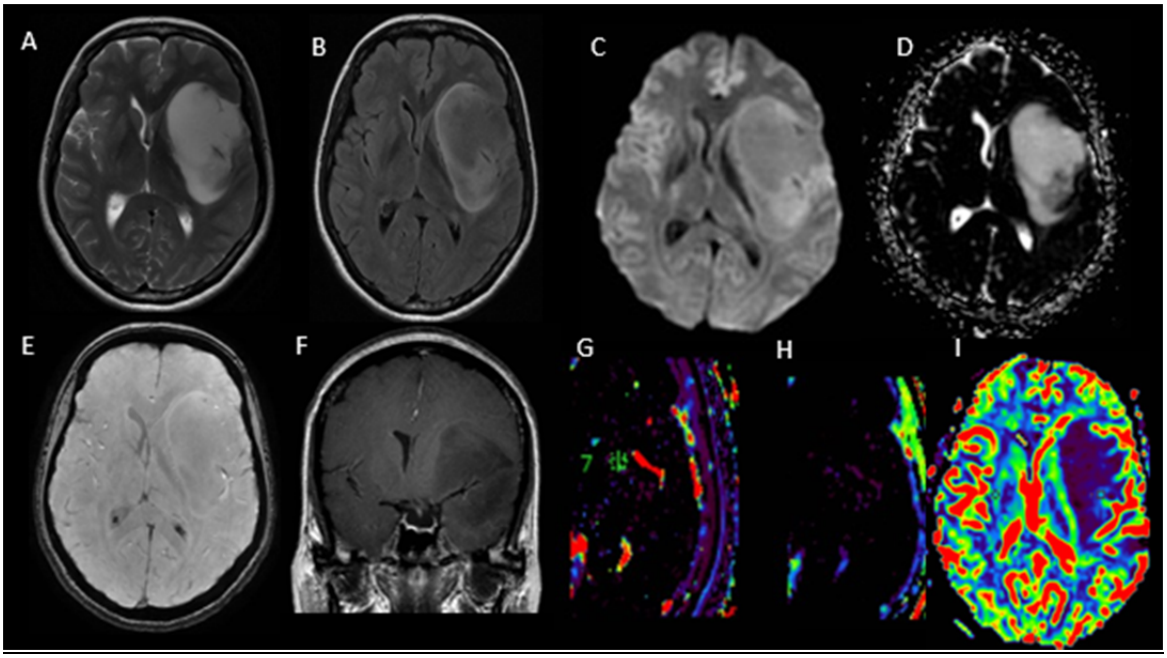

Fig 1: T2WI (A) and FLAIR (B) clearly demonstrate the FLAIR mismatch sign in the well circumscribed intra-axial mass lesion epicentred in the left insular region. Small area appearing hyperintense on DWI (C) and hypointense on ADC (D) , consistent with diffusion restriction is noted in the posterior part of the lesion. No areas of blooming are noted in the SWI (SWAN ,E) images. The lesion shows no enhancement (F) , low values of k-trans (G) , Ve (H) and rCBV (I) on MR perfusion.

Location	rCBV	K-trans	Ve	HPE	IDH status	MVD
Left Insular	0.97	0.056	0.037	Diffuse astrocytoma (Grade 2)	IDH mutant	52.58

Imaging Impression : Left Insular Low grade Glioma

Final integrated diagnosis : Diffuse astrocytoma, IDH Mutant, WHO grade II, Left Insula

CASE 2

42–year- male presented with recurrent headache over 03 month duration.

The MR Imaging (Fig 2) show well circumscribed lesion epicentred in the left peritrigonal and medial temporal lobe region.

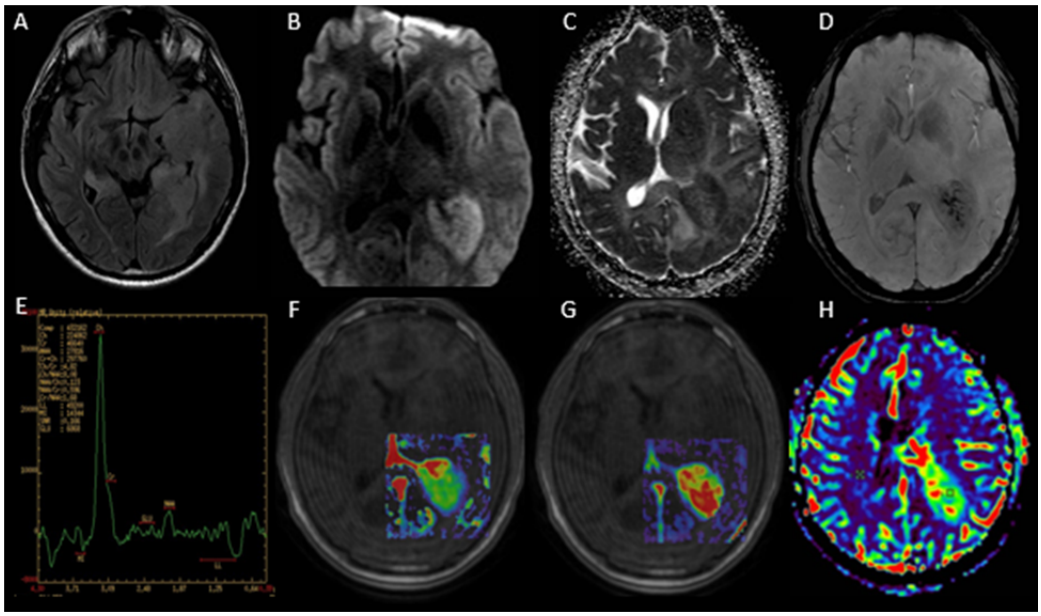

Fig 2 : FLAIR (A) demonstrate FLAIR hyperintense solid appearing intra-axial lesion involving the left peritrigonal and medial temporal lobe region. Most part of the lesion appear hyperintense on DWI (B) and hypointense on ADC (C) , consistent with diffusion restriction. A few foci of blooming are noted in the SWI (SWAN , D) images. The MR Spectroscopy (E) show markedly elevated Choline and reduced NAA. Significantly increased values of k-trans (F) , Ve (G) and rCBV (H) are noted on MR perfusion.

Location	rCBV	K-trans	Ve	HPE	IDH status	MVD
left peritrigonal	6.63	0.120	0.209	GBM	IDH mutant	133.17

Imaging Impression : Left temporal high grade Glioma

Final integrated diagnosis : Gliobastoma, IDH Mutant, WHO grade IV, Left temporal lobe

CASE 3

41–year- male presented with recurrent headache and focal seizure involving the left upper and Lower limbs over 02 month duration.

The MR Imaging (Fig 3) show well defined lesion epicentred in the right superior frontal gyrus.

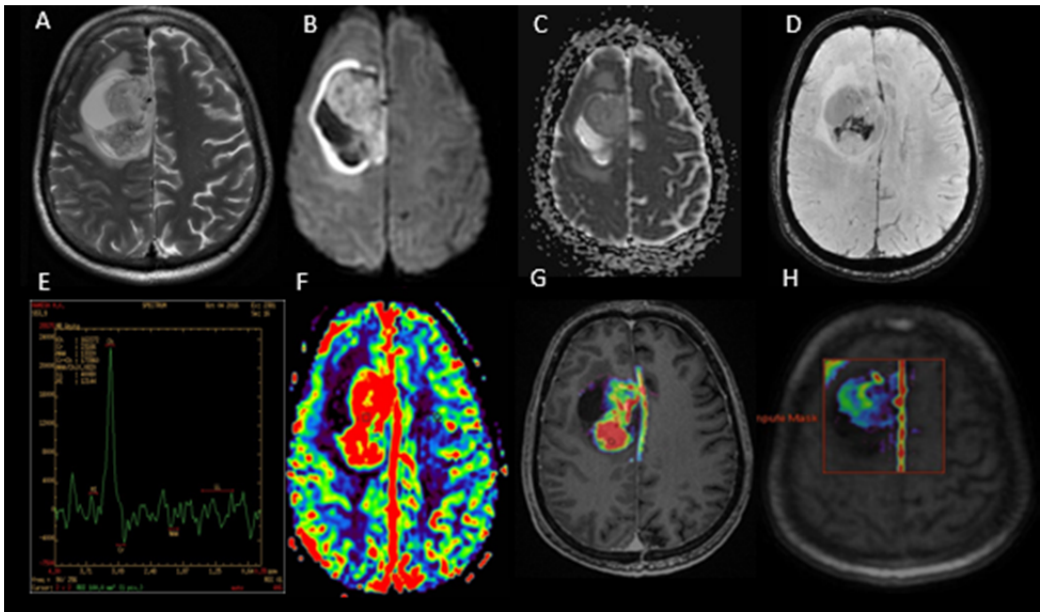

Fig 3 : T2WI (A) demonstrate a heterogeneously hyperintense mixed solid and cystic appearing intra-axial lesion epicentred in the right superior frontal gyrus region. Most part of the lesion appear markedly hyperintense on DWI (B) and iso to mildly hypointense on ADC (C) , consistent with diffusion restriction. A few foci of blooming are notedwithin the lesion on SWI (SWAN , D) images. The MR Spectroscopy (E) show markedly elevated Choline and reduced NAA. Significantly increased values of r-CBV(F) , k-trans (G) and Ve (H) are noted on MR perfusion.

Location	rCBV	K-trans	Ve	HPE	IDH status	MVD
Right frontal	7.86	0.381	0.066	AA	IDH Wild	182.31

Imaging Impression : Right temporal high grade Glioma

Final integrated diagnosis : Analastic astrocytoma, IDH Wild, WHO grade III, right frontal lobe

CASE 4

60–year- male presented with recurrent headache and altered behavior of 01 month duration.

The MR Imaging (Fig 4) show solid intraxial mass lesion epicentred in the genu of corpus callosum.

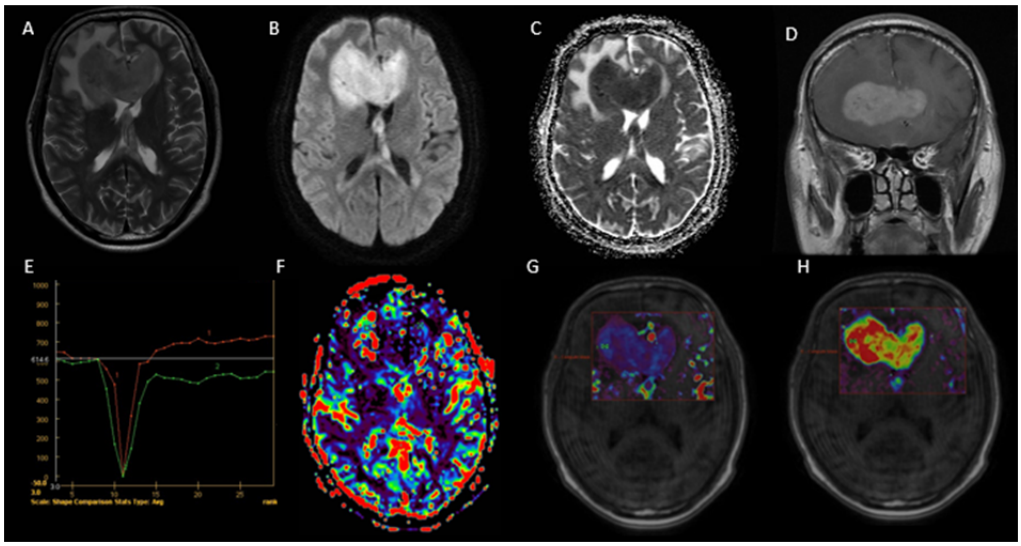

Fig 4 : T2WI (A) images demonstrate a T2 iso to hypointense solid intra-axial lesion epicentred in the genu of corpus callosum. Almost whole of the lesion appear markedly hyperintense on DWI (B) and hypointense on ADC (C) , consistent with diffusion restriction. The lesion shows homogeneous postcontrast enhancement with no evidence of cystic/necrotic appearing areas (D). The mean curve of DSC perfusion shows rapid signal overshoot above the baseline (E). Mild increase in rCBV values is noted on DSC perfusion. Significantly increased values of, k-trans (G) and Ve (H) are observed on DCE MR perfusion.

Location	rCBV	K-trans	Ve	HPE	IHC
Right Frontal	1.12	0.252	0.821	DLBCL	CD20 positive

Imaging Impression : Primary CNS Lymphoma

Final diagnosis : Diffuse large B-cell Lymphoma , corpus callosum and right frontal lobe

CASE 5

65–year-female presented with recurrent headache, vomiting and gait unsteadiness over 02 month duration.

The MR Imaging (Fig 5) show well circumscribed lesion epicentred in the right temporal lobe region.

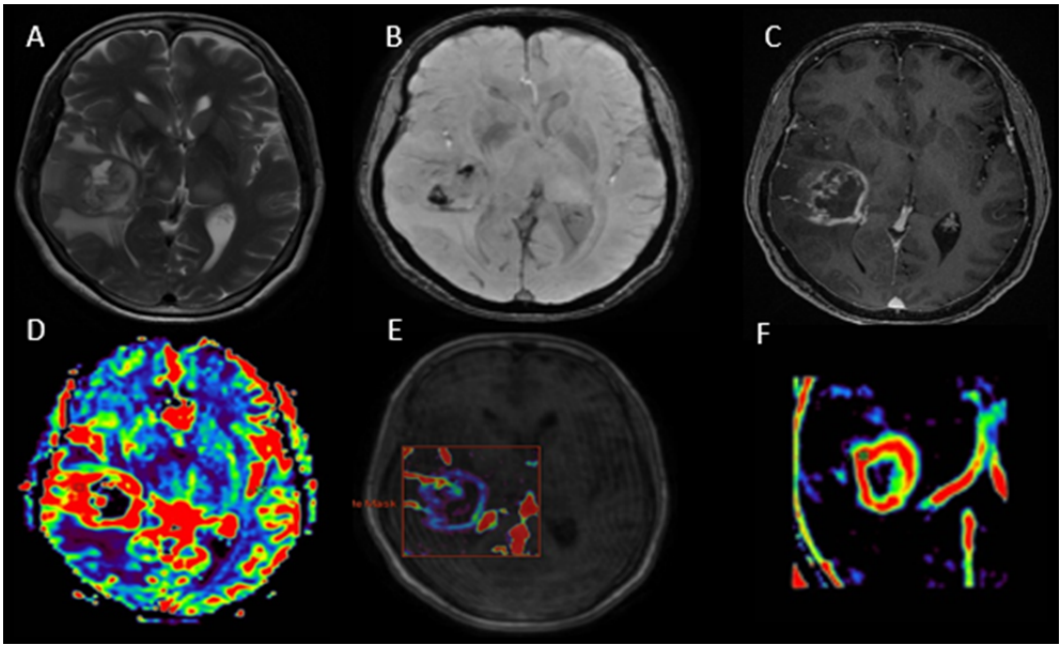

Fig 5 : T2WI (A) demonstrate heterogeneous intensity intra-axial lesion involving the right temporal lobe region. A few foci of blooming are noted within the lesion on SWI (SWAN , B) images. The postcontrast images show irregular nodular rim enhancement (C) . Significantly increase in rCBV (D) , k-trans (E) , and Ve (F) values is noted on MR perfusion.

Location	rCBV	K-trans	Ve	HPE	IDH status	MVD
Right Temporal	5.34	0.322	0.271	GBM	Wild	121.38

Impression : Right temporal high grade Glioma

Final integrated diagnosis : Gliobastoma, IDH wild , WHO grade IV, right temporal lobe

CASE 6

20–year- male presented with headache and vomiting over 06 month duration.

The MR Imaging (Fig 6) show well circumscribed lesion epicentred in the right thalamus region.

Location	rCBV	K-trans	Ve	HPE	IHC	MVD
Right thalamus	3.93	0.264	0.454	DMG	H3K27M	54.05

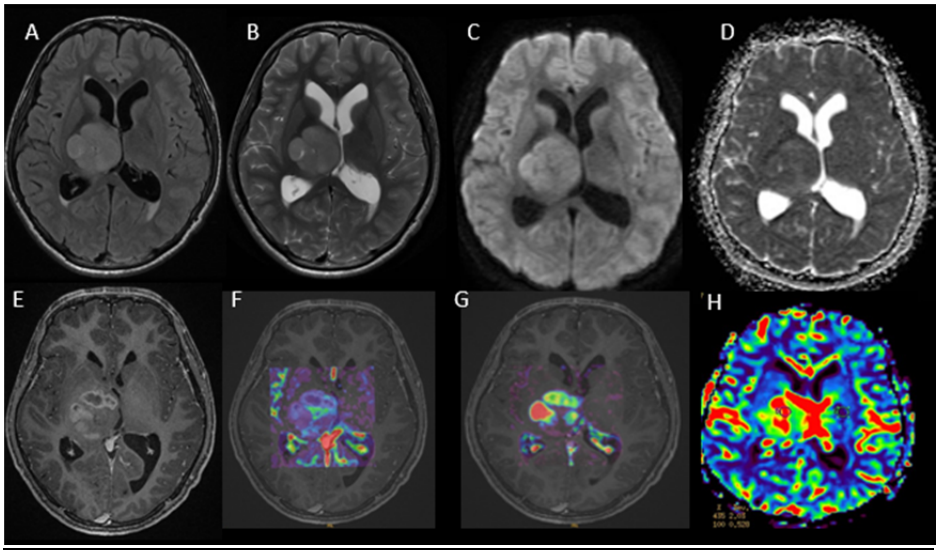

Fig 1: FLAIR (A) and T2WI (B) demonstrate the well circumscribed intra-axial mass lesion epicentred in the right thalamic region. No areas of diffusion restriction noted in the lesion(C,D). The lesion shows areas of peripheral enhancement with few central non enhancing areas within (E) , high values of k-trans (F) , Ve (G) and rCBV (H) on MR perfusion.

Impression : Right thalamic diffuse pontine glioma

Final integrated diagnosis : Right Thalamic diffuse pontine glioma

Discussion

DISCUSSION

A total of 52 patients with intraxial brain masses fulfilling the inclusion criteria were identified and evaluated in the study. Among the cases included in our study, 30 were male and the rest (22/52) were female.

46 of the total 52 patients underwent HPE evaluation and were classified according to 2016 WHO Classification of Tumors of the Central Nervous System.

The HPE evaluated cases comprised two WHO grade II (2/46, 4.3%), 24 WHO grade III (52.1%) , 17 WHO grade IV tumors (36.9%) and 3 cases of PCNSL(6.5%). The 6 of the 8 cases of low grade glioma included in the study did not undergo HPE and were assumed to be grade 2 based on the stable low values of k-trans, Ve , Kep and rCBV over 2 years. Cases which showed HPE features suggestive of oligodendroglioma and demonstrated no loss of ATRX did not undergo evaluation for 1p 19q status and were labelled as oligodendroglioma NOS.

The WHO grade IV tumors included: glioblastoma (13/17, 76.4%) and diffuse midline glioma H3 K27M mutant (4/17, 23.5%). Of the 13 Glioblastoma cases, IDH-wildtype comprised 11 (11/13, 84.6%) and the IDH-mutant type comprised 2 (2/13, 15.3%) .

The WHO grade III tumors included 9 cases of IDH-mutant anaplastic astrocytoma, (9/24, 37.5%), 7 cases of anaplastic astrocytoma NOS (7/24, 29.1%) and 8 cases of anaplastic oligodendroglioma NOS (8/24, 33.3%). The both cases of HPE proven WHO grade II tumor were IDH-mutant diffuse astrocytoma.

The HPE was done on the excised sample in all cases of AODG, and one but all cases of AA and GB. All DMG and one but all cases of PCNSL underwent HPE evaluation following biopsy.

LGG versus HGG:

The DCE perfusion parameters (k-trans and Ve) as well as DSC perfusion parameter (rCBV) showed statistically significant differences in parametric values in differentiating the LGG and HGG. Although k-trans , Ve and rCBV all reached statistical significance, the later achieved the maximum statistical significance.

Within the independent parametric variables the area was highest for rCBV (0.938), though similarly high AUC values were seen for K-trans and Ve (0.848 and 0.867 respectively).

In our study, K-trans Cut-off value of 0.080 differentiated LGG from HGG with a sensitivity of 64.8 % and specificity of 100%. Also, k-trans Cut-off value of 0.056 differentiated LGG from HGG with a sensitivity of 78.38 % and specificity of 75 %. Ve Cut-off value of 0.037 differentiated LGG from HGG with a sensitivity of 75.68 % and specificity of 100%.

The most DCE studies show increasing K trans and Ve values with progressive tumor grade**.** [17,62,73] However the K trans , Ve and Vp cut-off values differ markedly among studies ,emphasing the need to consider various confounding factors (type of pharmacokinetic model, contrast agent and T10 among others) while comparing the results among two studies. Takashi et al found cutoff value of Ktrans = 0.0848 and Ve =0.18 provided the best good combination of sensitivity and specificity for diagnosis of LGG**.** [36] These values of ktrans and Ve yield sensitivity and specificity (088% and 100%) and (96% and 100%) respectively.

Corrado Santarosa et al documented sensitivity and specificity of 100% for both the Vp (max) cut-off value of 2.25 mL/100 and K trans (max) cut-off value of 0.019.[12] Li et al found cutoff value of Ktrans = 0.054 and Ve =0.296 provided the best good combination of sensitivity and specificity for differentiation for LGG from HGG. These values of ktrans and Ve yield sensitivity and specificity (94.1% and 93.3%) and (92.9% and 91.7%) respectively.[58]

Tufail F et al demonstrated close correlation between k-trans, vp and rCBV and attributed this close correlation to the observation that Ktrans is directly affected not merely by endothelial permeability surface area product(PSAP), but also by blood flow.[11]

The results from various studies which examined relationship between the k-trans and rCBV with tumor grade observed varying degree of correlation between the two. Although many studies documented strong correlation, others observed a weak correlation and documented rCBV to be a more accurate parameter compared to k-trans in tumor grading.[52] Similarly poor correlation between k-trans and blood flow parameters (Vp and rCBV) has been observed by other authors.[12] The wide variation in the methodology may be an important factor contributing to the observed varying degree of correlation between various studies and highlights the importance of validated and standardized pharmacokinetic modeling technique in accurate tumor grading with DCE MR.

A few studies failed to demonstrate any relationship between tumor grade and K-trans or at best demonstrated only a weak relationship.[52,74]

In our study , The rCBV Cut-off value of 1.28 differentiated LGG from HGG with a sensitivity of 86.49 % and specificity of 100%. Also, rCBV Cut-off value of 1.13 differentiated LGG from HGG with a sensitivity of 94.59 % and specificity of 75%.

No universally agreeable rCBV threshold exists to differentiate HGN from LGN , with Ji Hoon Shin et al , Nail Bulakbasi et al, Meng Law et al and Riyadh N et al suggesting rCBV cut-off values of 2.93, 2.60, 1.75 and 1.75, respectively**.** [50-53] Glioma with high rCBV, specifically more than 1.75 progress faster and are associated with a poor prognosis**.** [52] Friso W. A observed sensitivity and specificity of 70% and 100% respectively for the rCBVmax cut-off values of 1.85**.** [15]

Grade III versus Grade IV Glioma : ROC curve (K trans, Ve and rCBV)

In our study , k-trans Cut-off value of 0.072 provided the best good combination of sensitivity and specificity (92.31% and 45.83 respectively) for differentiating grade III from grade IV. Ve Cut-off value of 0.112 provided the best good combination of sensitivity and specificity (100% and 79.17% respectively) for differentiating grade III from grade IV. rCBV Cut-off value of 3.46 differentiated grade III from grade IV with a sensitivity of 92.31 % and specificity of 62.50%. Within the independent parametric variables the AUC was highest for Ve (0.912), with AUC noted for rCBV and K-trans as 0.768 and 0.583 respectively.

Similar to our study, study by Corrado Santarosa et al relating to cut-off for differentiation of each glioma grade separately , found highly significant positive correlation of tumour grade with k-trans, Vp and rCBV and highest correlation was noted for Ve (Spearman's rank correlation coefficients of 0.795 for mean Vp , 0.702 for Ktrans and of 0.705 for mean rCBV) **.** [12]

Also , Li et al in their study found that although mean Ktrans and Ve values of grade III/IV gliomas were significantly higher than those of grade II gliomas, no significant differences were found between grade III and IV gliomas.[58]

Grade II versus Grade III Glioma : ROC curve (K trans, Ve and rCBV)

In our study, k-trans Cut-off value of 0.052 provided the best good combination of sensitivity and specificity (83.33% and 75.0 respectively) for differentiating grade II from grade III glial tumors. Ve Cut-off value of 0.025 differentiated grade II from grade III with a sensitivity of 75 % and specificity of 87.50%. rCBV Cut-off value of 1.28 provided the best good combination of sensitivity and specificity (79.17 % and 100% respectively) for differentiating grade II from grade III glial tumors.

Within the independent parametric variables, the AUC was highest for rCBV (0.904), with AUC noted for K-trans and Ve as 0.711 and 0.794 respectively.

Li et al used a cut-off values of Ktrans = 0.045 and Ve = 0.296 for differentiation between grade II and grade III gliomas with a high sensitivity and specificity (> 85%). [58] Other studies with similar observation and highlighting role of DCE and DSC perfusion parameters in differentiating between gd II and gd III are documented in the literature. [12,75]

MVD assessment:

Microvascular proliferation , a crucial characteristic of HGG , predicts glioma grade, prognosis and treatment response. The increase in the degree of proliferation of such immature vessels is noted to correspond strongly with progressive tumour grade. [76,77] In our study, the mean microvessel density (MVD) was 114.7/mm^2 (WHO grade III tumors) , 141.5/mm^2 (WHO grade IV tumors) , 110.5/mm^2 (IDH-mutant anaplastic astrocytoma) , 104.2/mm^2 (anaplastic astrocytoma NOS), 129.3/mm^2 (anaplastic

oligodendroglioma, NOS) and 79.1/mm^2 (diffuse midline glioma H3 K27M-mutant). The Pearson correlation coefficient between MCD and k-trans , MCD and Ve and between MCD and rCBV was 0.445, 0.017 and 0.522 respectively (Table 14) . The Pearson correlation coefficient shows moderate positive correlation between MVD and rCBV , intermediate correlation with K-trans and and a poor correlation using the Ve. Although higher mean MVD was noted in GBM compared to grade III tumors (AODG, AA), no statistically significant differences in MVD was noted between these two groups.

In our study, relatively higher rCBV values were noted in AODG compared to AA. Similarly, higher rCBV in oligodendroglioma (compared to anaplastic astrocytoma) have been noted by authors and is attributed to also to its predominant cortical location(and therefore prominent susceptibility variations from adjacent cortical macro-vessels and venous vessel) and not merely to its unique “chickenwire” microvessel network pattern**.** [60]

The study by Zhong et al showed statistically significant differences between HGG and LGG with respect to Ktrans, Ve and CD105-MVD values. The values in LGG were significantly lower than those of HGG (grade III and IV). Although Ktrans and Ve positively correlated with MVD in HGG, no statistically significant differences in MVD was noted between grade III and IV gliomas**.** [73]

Yao et al in their study concluded that MVD assessment using CD105 is more accurate in comparision to utilizing CD 34 for its assessment**.** [78]

Li et al observed that Ve values weakly correlated with MVD but moderately correlated with microveesel diameter (VD) values and concluded that VD values greatly influence the Ve values in Gliomas.[58]

Oligodendrogliomas showed higher MVD but smaller VD values whereas both the parameters (MVD and VD) were higher in HGGs.[58]

Primary central nervous system lymphoma (PCNSL) : The marked difference in the management strategy between the PCNSL and GBM makes the preoperative differentiation of the two highly relevant.[61]

In our study, the PCNSL showed mean k-trans = 0.204 (varied from 0.137 to 0.252), Ve = 0.516 (varied from 0.266 to 0.821) and the rCBV = 5.84 (varied from 1.04 to 10.32). The mean k-trans , Ve and the rCBV in our GBM cases was 0.28 , 0.33 and 6.09. Although the Ve values were notably higher in PCNSL, there existed a significant overlap between the two disease processes. Similarly the k-trans and rCBV showed significant overlap between GBM and PCNSL.

Similarly, Permeability indices, including Ktrans, have been shown in number of earlier studies to correlate with glioma grade but to overlap with Lymphoma.[62,17]

However, Kickingereder et al observed significantly higher k-trans and kep values in PCNSL compared to GBM (but no difference in Ve values)and also noted sensitivity of 90.9% and specificity of 95.0% using the k-trans cut-off value of 0.093. The higher k-trans and kep values in PCNSL (compared to GBM) may be attributed to less flow limited behavior to the contrast agent uptake in the former.[59]

Due to the difference in the degree of neovascularization between the PCNSL and GBM, most of the studies show significantly lower rCBV values in the former compared to the latter.[48,63]

The higher values of rCBV in our cases can be partly attributed to the preloading of contrast before the MR DSC scan. The CBV without contrast leakage correction seems to have the best diagnostic performance in differentiating the PCNSL and GBM.[48]

Diffuse midline Glioma (**DMG**) :

In our study , All DMG were evaluated with HPE (biopsy sample) and confirmed following H3 K27M mutant status evaluation. The all four cases were noted centred in the right thalamus with average age at presentation of 28 years and showed high MR perfusion parameters (k-trans, Ve and rCBV). The average k-trans value noted was 0.285 (varied from 0.080 to 0.446) , average Ve = 0.291 (varied from 0.046 to 0.454) and the average rCBV = 6.37 (varied from 3.93 to 12.34).

These tumors show predilection for thalamus, pons and spinal cord , are predominantly noted in children or young adult and are categorized as grade IV tumors , regardless of histological features.[69] Similar to our cases , the retrospective analyses of 47 cases of DMG tumors showed average age of 24 years in those with thalamus epicentred lesions.[69] However, patients with pontine gliomas tend to be younger (median age 7 years). The Pons and thalamus are the two most common sites to be involved in DMG.[68,69] Although sufficient data on the MR perfusion in DMG is lacking , the lesions are characterized as grade IV tumour and are expected to show significantly increased MR perfusion.

Limitations of study

The important limitations of this prospective study comprise less number of histopathologically proven low grade glioma , non assessment of 1p19q mutation status for confirming diagnosis of oligodendroglioma and grade wise relatively smaller number of patients and thus statistical power to detect such difference was weak.

Conclusion

CONCLUSION:

DSC technique , the most widely used and time tested MR perfusion method remains the most robust and widely used parameter with a few disadvantages (difficulty in determining absolute quantification, presence of susceptibility artefacts and the invalid assumption of BBB integrity in DSC imaging).

We demonstrated the utility of DCE-MRI in the differential diagnosis of intraxial brain tumors using commercially available software (incorporating automatic vascular function detection and a fixed T1 method) and therefore high feasibility for its clinical use.

Ktrans , Ve and rCBV parameters showed higher values with increasing glioma grades. All measurements show good discriminative power in distinguishing between low- and high-grade gliomas. However, the parameters were not as accurate in differentiating grade III from grade IV or grade II from III tumours.

The more accurate results were obtained with DCE parameters in tumours showing increased suscebtibilty (calcification and haemorrhage).

The cases of lymphoma showed overlapping MR perfusion values (including rCBV) with Glioblastoma.

The microvessel density , tumour grade and MR perfusion parameters (k-trans, Ve and rCBV) showed moderate positive correlation with rCBV noted to be most closely related to MVD among all MR perfusion parameters.

References

REFERENCES

1. Lacerda S, Law M. Magnetic Resonance Perfusion and Permeability Imaging in Brain Tumors. Neuroimaging Clin N Am. 2009 Nov;19(4):527–57.

2. Essig M, Shiroishi MS, Nguyen TB, Saake M, Provenzale JM, Enterline D, et al. Perfusion MRI: The Five Most Frequently Asked Technical Questions. Am J Roentgenol. 2013 Jan;200(1):24–34.

3. Kimura M, da Cruz LCH. Multiparametric MR Imaging in the Assessment of Brain Tumors. Magn Reson Imaging Clin N Am. 2016 Feb;24(1):87–122.

4. Jain R, Gutierrez J, Narang J, Scarpace L, Schultz LR, Lemke N, et al. In Vivo Correlation of Tumor Blood Volume and Permeability with Histologic and Molecular Angiogenic Markers in Gliomas. Am J Neuroradiol. 2011 Feb;32(2):388–94.

5. Jiang W, Huang Y, An Y, Kim BYS. Remodeling Tumor Vasculature to Enhance Delivery of Intermediate-Sized Nanoparticles. ACS Nano. 2015 Sep 22;9(9):8689–96.

6. Wen PY, Macdonald DR, Reardon DA, Cloughesy TF, Sorensen AG, Galanis E, et al. Updated Response Assessment Criteria for High-Grade Gliomas: Response Assessment in Neuro-Oncology Working Group. J Clin Oncol. 2010 Apr 10;28(11):1963–72.

7. Johnson DR, Guerin JB, Giannini C, Morris JM, Eckel LJ, Kaufmann TJ. 2016 Updates to the WHO Brain Tumor Classification System: What the Radiologist Needs to Know. RadioGraphics. 2017 Nov;37(7):2164–80.

8. Pope WB, Sayre J, Perlina A, Villablanca JP, Mischel PS, Cloughesy TF. MR Imaging Correlates of Survival in Patients with High-Grade Gliomas. 2005;9.

9. Chaichana KL, McGirt MJ, Niranjan A, Olivi A, Burger PC, Quinones-Hinojosa A. Prognostic significance of contrast-enhancing low-grade gliomas in adults and a review of the literature. Neurol Res. 2009 Nov;31(9):931–9.

10. Barker FG, Chang SM, Huhn SL, Davis RL, Gutin PH, McDermott MW, et al. Age and the risk of anaplasia in magnetic resonance-nonenhancing supratentorial cerebral tumors. Cancer. 1997 Sep 1;80(5):936–41.

11. Patankar TF, Haroon HA, Mills SJ, Baleriaux D, Buckley DL, Parker GJM, et al. Is Volume Transfer Coefficient (Ktrans) Related to Histologic Grade in Human Gliomas? 2005;11.

12. Santarosa C, Castellano A, Conte GM, Cadioli M, Iadanza A, Terreni MR, et al. Dynamic contrast-enhanced and dynamic susceptibility contrast perfusion MR imaging for glioma grading: Preliminary comparison of vessel compartment and permeability parameters using hotspot and histogram analysis. Eur J Radiol. 2016 Jun;85(6):1147–56.

13. Jahng G-H, Li K-L, Ostergaard L, Calamante F. Perfusion Magnetic Resonance Imaging: A Comprehensive Update on Principles and Techniques. Korean J Radiol. 2014;15(5):554.

14. Petrella JR, Provenzale JM. MR Perfusion Imaging of the Brain: Techniques and Applications. Am J Roentgenol. 2000 Jul;175(1):207–19.

15. Hoefnagels FWA, Lagerwaard FJ, Sanchez E, Haasbeek CJA, Knol DL, Slotman BJ, et al. Radiological progression of cerebral metastases after radiosurgery:

assessment of perfusion MRI for differentiating between necrosis and recurrence. J Neurol. 2009 Jun;256(6):878–87.

16. Tofts PS, Brix G, Buckley DL, Evelhoch JL, Henderson E, Knopp MV, et al. Estimating kinetic parameters from dynamic contrast-enhanced t1-weighted MRI of a diffusable tracer: Standardized quantities and symbols. J Magn Reson Imaging. 1999 Sep;10(3):223–32.

17. Zhang Y, Wang J, Wang X, Zhang J, Fang J, Jiang X. Feasibility study of exploring a T1-weighted dynamic contrast-enhanced MR approach for brain perfusion imaging. J Magn Reson Imaging. 2012 Jun;35(6):1322–31.

18. Artzi M, Liberman G, Nadav G, Vitinshtein F, Blumenthal DT, Bokstein F, et al. Human cerebral blood volume measurements using dynamic contrast enhancement in comparison to dynamic susceptibility contrast MRI. Neuroradiology. 2015 Jul;57(7):671–8.

19. Abbott NJ, Friedman A. Overview and introduction: The blood-brain barrier in health and disease: Blood-Brain Barrier in Health and Disease. Epilepsia. 2012 Nov;53:1–6.

20. Obermeier B, Daneman R, Ransohoff RM. Development, maintenance and disruption of the blood-brain barrier. Nat Med. 2013 Dec;19(12):1584–96.

21. Singh IN, Sullivan PG, Hall ED. Peroxynitrite-mediated oxidative damage to brain mitochondria: Protective effects of peroxynitrite scavengers. J Neurosci Res. 2007 Aug 1;85(10):2216–23.

22. Armitage P, Behrenbruch C, Brady M, Moore N. Extracting and visualizing physiological parameters using dynamic contrast-enhanced magnetic resonance imaging of the breast. Med Image Anal. 2005 Aug;9(4):315–29.

23. Armitage PA, Farrall AJ, Carpenter TK, Doubal FN, Wardlaw JM. Use of dynamic contrast-enhanced MRI to measure subtle blood–brain barrier abnormalities. Magn Reson Imaging. 2011 Apr;29(3):305–14.

24. Heye AK, Culling RD, Valdés Hernández M del C, Thrippleton MJ, Wardlaw JM. Assessment of blood–brain barrier disruption using dynamic contrast-enhanced MRI. A systematic review. NeuroImage Clin. 2014;6:262–74.

25. Jelescu IO, Leppert IR, Narayanan S, Araújo D, Arnold DL, Pike GB. Dual-temporal resolution dynamic contrast-enhanced MRI protocol for blood-brain barrier permeability measurement in enhancing multiple sclerosis lesions. J Magn Reson Imaging. 2011 Jun;33(6):1291–300.

26. Li K-L, Buonaccorsi G, Thompson G, Cain JR, Watkins A, Russell D, et al. An improved coverage and spatial resolution-using dual injection dynamic contrast-enhanced (ICE-DICE) MRI: A novel dynamic contrast-enhanced technique for cerebral tumors. Magn Reson Med. 2012 Aug;68(2):452–62.

27. Miyati T, Banno T, Mase M, Kasai H, Shundo H, Imazawa M, et al. Dual dynamic contrast-enhanced MR imaging. J Magn Reson Imaging. 1997 Jan;7(1):230–5.

28. Thompson EM, Guillaume DJ, Dósa E, Li X, Nazemi KJ, Gahramanov S, et al. Dual contrast perfusion MRI in a single imaging session for assessment of pediatric brain tumors. J Neurooncol. 2012 Aug;109(1):105–14.

29. Schabel MC, Parker DL. Uncertainty and bias in contrast concentration measurements using spoiled gradient echo pulse sequences. Phys Med Biol. 2008 May 7;53(9):2345–73.

30. Brookes JA, Redpath TW, Gilbert FJ, Murray AD, Staff RT. Accuracy of T1 measurement in dynamic contrast-enhanced breast MRI using two- and three-dimensional variable flip angle fast low-angle shot. J Magn Reson Imaging. 1999 Feb;9(2):163–71.

31. Lavini C, Verhoeff JJC. Reproducibility of the gadolinium concentration measurements and of the fitting parameters of the vascular input function in the superior sagittal sinus in a patient population. Magn Reson Imaging. 2010 Dec;28(10):1420–30.

32. Calamante F. Arterial input function in perfusion MRI: A comprehensive review. Prog Nucl Magn Reson Spectrosc. 2013 Oct;74:1–32.

33. You S-H, Choi SH, Kim TM, Park C-K, Park S-H, Won J-K, et al. Differentiation of High-Grade from Low-Grade Astrocytoma: Improvement in Diagnostic Accuracy and Reliability of Pharmacokinetic Parameters from DCE MR Imaging by Using Arterial Input Functions Obtained from DSC MR Imaging. Radiology. 2018 Mar;286(3):981–91.

34. Sourbron SP, Buckley DL. Classic models for dynamic contrast-enhanced MRI: CLASSIC MODELS FOR DCE-MRI. NMR Biomed. 2013 Aug;26(8):1004–27.

35. Larsson HBW, Courivaud F, Rostrup E, Hansen AE. Measurement of brain perfusion, blood volume, and blood-brain barrier permeability, using dynamic contrast-enhanced T_1-weighted MRI at 3 tesla. Magn Reson Med. 2009 Nov;62(5):1270–81.

36. Abe T, Mizobuchi Y, Nakajima K, Otomi Y, Irahara S, Obama Y, et al. Diagnosis of brain tumors using dynamic contrast-enhanced perfusion imaging

with a short acquisition time. SpringerPlus [Internet]. 2015 Dec [cited 2018 Jul 27];4(1). Available from: http://www.springerplus.com/content/4/1/88

37. Harrer JU, Parker GJM, Haroon HA, Buckley DL, Embelton K, Roberts C, et al. Comparative study of methods for determining vascular permeability and blood volume in human gliomas: Assessment of Vascular Permeability. J Magn Reson Imaging. 2004 Nov;20(5):748–57.

38. Budde MD, Gold E, Jordan EK, Frank JA. Differential microstructure and physiology of brain and bone metastases in a rat breast cancer model by diffusion and dynamic contrast enhanced MRI. Clin Exp Metastasis. 2012 Jan;29(1):51–62.

39. Sourbron SP, Buckley DL. On the scope and interpretation of the Tofts models for DCE-MRI. Magn Reson Med. 2011 Sep;66(3):735–45.

40. Cramer SP, Larsson HB. Accurate Determination of Blood–Brain Barrier Permeability Using Dynamic Contrast-Enhanced T1-Weighted MRI: A Simulation and in vivo Study on Healthy Subjects and Multiple Sclerosis Patients. J Cereb Blood Flow Metab. 2014 Oct;34(10):1655–65.

41. Tofts PS, Kermode AG. Measurement of the blood-brain barrier permeability and leakage space using dynamic MR imaging. 1. Fundamental concepts. Magn Reson Med. 1991 Feb;17(2):357–67.

42. Ewing JR, Bagher-Ebadian H. Model selection in measures of vascular parameters using dynamic contrast-enhanced MRI: experimental and clinical applications: model selection in dynamic contrast-enhanced MRI. NMR Biomed. 2013 Aug;26(8):1028–41.

43. Rosen BR, Belliveau JW, Buchbinder BR, McKinstry RC, Porkka LM, Kennedy DN, et al. Contrast agents and cerebral hemodynamics. Magn Reson Med. 1991 Jun;19(2):285–92.

44. Boxerman JL, Prah DE, Paulson ES, Machan JT, Bedekar D, Schmainda KM. The Role of Preload and Leakage Correction in Gadolinium-Based Cerebral Blood Volume Estimation Determined by Comparison with MION as a Criterion Standard. Am J Neuroradiol. 2012 Jun;33(6):1081–7.

45. Sadeghi N, D'Haene N, Decaestecker C, Levivier M, Metens T, Maris C, et al. Apparent Diffusion Coefficient and Cerebral Blood Volume in Brain Gliomas: Relation to Tumor Cell Density and Tumor Microvessel Density Based on Stereotactic Biopsies. Am J Neuroradiol. 2008 Mar;29(3):476–82.

46. Floriano VH, Torres US, Spotti AR, Ferraz-Filho JRL, Tognola WA. The Role of Dynamic Susceptibility Contrast-Enhanced Perfusion MR Imaging in Differentiating between Infectious and Neoplastic Focal Brain Lesions: Results from a Cohort of 100 Consecutive Patients. Harel N, editor. PLoS ONE. 2013 Dec 6;8(12):e81509.

47. Hakyemez B, Erdogan C, Bolca N, Yildirim N, Gokalp G, Parlak M. Evaluation of different cerebral mass lesions by perfusion-weighted MR imaging. J Magn Reson Imaging. 2006 Oct;24(4):817–24.

48. Toh CH, Wei K-C, Chang C-N, Ng S-H, Wong H-F, Lin C-P. Differentiation of Brain Abscesses from Glioblastomas and Metastatic Brain Tumors: Comparisons of Diagnostic Performance of Dynamic Susceptibility Contrast-Enhanced Perfusion MR Imaging before and after Mathematic Contrast Leakage Correction. Sherman J, editor. PLoS ONE. 2014 Oct 17;9(10):e109172.

49. Hourani R, Brant LJ, Rizk T, Weingart JD, Barker PB, Horska A. Can Proton MR Spectroscopic and Perfusion Imaging Differentiate Between Neoplastic and Nonneoplastic Brain Lesions in Adults? Am J Neuroradiol. 2008 Feb 1;29(2):366–72.

50. Shin JH, Lee HK, Kwun BD, Kim J-S, Kang W, Choi CG, et al. Using Relative Cerebral Blood Flow and Volume to Evaluate the Histopathologic Grade of Cerebral Gliomas: Preliminary Results. Am J Roentgenol. 2002 Sep;179(3):783–9.

51. Bulakbasi N, Kocaoglu M, Farzaliyev A, Tayfun C, Ucoz T, Somuncu I. Assessment of Diagnostic Accuracy of Perfusion MR Imaging in Primary and Metastatic Solitary Malignant Brain Tumors. 2005;13.

52. Law M, Yang S, Babb JS, Knopp EA, Golfinos JG, Zagzag D, et al. Comparison of Cerebral Blood Volume and Vascular Permeability from Dynamic Susceptibility Contrast-Enhanced Perfusion MR Imaging with Glioma Grade. 2004;10.

53. Al-Okaili RN, Krejza J, Woo JH, Wolf RL, O'Rourke DM, Judy KD, et al. Intraaxial Brain Masses: MR Imaging–based Diagnostic Strategy—Initial Experience. Radiology. 2007 May;243(2):539–50.

54. Hu LS, Kelm Z, Korfiatis P, Dueck AC, Elrod C, Ellingson BM, et al. Impact of Software Modeling on the Accuracy of Perfusion MRI in Glioma. Am J Neuroradiol. 2015 Dec;36(12):2242–9.

55. Toh CH, Wei K-C, Chang C-N, Ng S-H, Wong H-F. Differentiation of Primary Central Nervous System Lymphomas and Glioblastomas: Comparisons of Diagnostic Performance of Dynamic Susceptibility Contrast-Enhanced Perfusion

MR Imaging without and with Contrast-Leakage Correction. Am J Neuroradiol. 2013 Jun;34(6):1145–9.

56. Law M. Advanced imaging techniques in brain tumors. Cancer Imaging. 2009;9(Special Issue A):S4–9.

57. Calli C, Kitis O, Yunten N, Yurtseven T, Islekel S, Akalin T. Perfusion and diffusion MR imaging in enhancing malignant cerebral tumors. Eur J Radiol. 2006 Jun;58(3):394–403.

58. Li X, Zhu Y, Kang H, Zhang Y, Liang H, Wang S, et al. Glioma grading by microvascular permeability parameters derived from dynamic contrast-enhanced MRI and intratumoral susceptibility signal on susceptibility weighted imaging. Cancer Imaging [Internet]. 2015 Dec [cited 2018 Jul 27];15(1). Available from: http://www.cancerimagingjournal.com/content/15/1/4

59. Kickingereder P, Wiestler B, Sahm F, Heiland S, Roethke M, Schlemmer H-P, et al. Primary Central Nervous System Lymphoma and Atypical Glioblastoma: Multiparametric Differentiation by Using Diffusion-, Perfusion-, and Susceptibility-weighted MR Imaging. Radiology. 2014 Sep;272(3):843–50.

60. Lev MH, Ozsunar Y, Henson JW, Rasheed AA, Barest GD, IV GRH, et al. Glial Tumor Grading and Outcome Prediction Using Dynamic Spin-Echo MR Susceptibility Mapping Compared with Conventional Contrast-Enhanced MR: Confounding Effect of Elevated rCBV of Oligodendroglimoas. 2004;8.

61. Schlegel U. Review: Primary CNS lymphoma. Ther Adv Neurol Disord. 2009 Mar;2(2):93–104.

62. Xyda A, Haberland U, Klotz E, Jung K, Bock HC, Schramm R, et al. Diagnostic performance of whole brain volume perfusion CT in intra-axial brain tumors:

Preoperative classification accuracy and histopathologic correlation. Eur J Radiol. 2012 Dec;81(12):4105–11.

63. Hartmann M, Heiland S, Harting I, Tronnier VM, Sommer C, Ludwig R, et al. Distinguishing of primary cerebral lymphoma from high-grade glioma with perfusion-weighted magnetic resonance imaging. Neurosci Lett. 2003 Feb;338(2):119–22.

64. Emblem KE, Bjornerud A, Mouridsen K, Borra RJ, Batchelor TT, Jain RK, et al. T_1 - and T_2 Dominant Extravasation Correction in DSC-MRI: Part II—Predicting Patient Outcome after a Single Dose of Cediranib in Recurrent Glioblastoma Patients. J Cereb Blood Flow Metab. 2011 Oct;31(10):2054–64.

65. Makino K, Hirai T, Nakamura H, Murakami R, Kitajima M, Shigematsu Y, et al. Does adding FDG-PET to MRI improve the differentiation between primary cerebral lymphoma and glioblastoma? Observer performance study. Ann Nucl Med. 2011 Jul;25(6):432–8.

66. Louis DN, Perry A, Burger P, Ellison DW, Reifenberger G, von Deimling A, et al. International Society of Neuropathology-Haarlem Consensus Guidelines for Nervous System Tumor Classification and Grading: ISN-Haarlem Brain Tumor Classification Guidelines. Brain Pathol. 2014 Sep;24(5):429–35.

67. Smits M, van den Bent MJ. Imaging Correlates of Adult Glioma Genotypes. Radiology. 2017 Aug;284(2):316–31.

68. Aboian MS, Solomon DA, Felton E, Mabray MC, Villanueva-Meyer JE, Mueller S, et al. Imaging Characteristics of Pediatric Diffuse Midline Gliomas with Histone H3 K27M Mutation. Am J Neuroradiol. 2017 Apr;38(4):795–800.

69. Solomon DA, Wood MD, Tihan T, Bollen AW, Gupta N, Phillips JJJ, et al. Diffuse Midline Gliomas with Histone H3-K27M Mutation: A Series of 47 Cases Assessing the Spectrum of Morphologic Variation and Associated Genetic Alterations: Diffuse midline gliomas with histone H3-K27M mutation. Brain Pathol. 2016 Sep;26(5):569–80.

70. St. Jude Children's Research Hospital–Washington University Pediatric Cancer Genome Project, Wu G, Broniscer A, McEachron TA, Lu C, Paugh BS, et al. Somatic histone H3 alterations in pediatric diffuse intrinsic pontine gliomas and non-brainstem glioblastomas. Nat Genet. 2012 Mar;44(3):251–3.

71. Aihara K, Mukasa A, Gotoh K, Saito K, Nagae G, Tsuji S, et al. H3F3A K27M mutations in thalamic gliomas from young adult patients. Neuro-Oncol. 2014 Jan;16(1):140–6.

72. Cai H, Xue Y, Liu W, Li Z, Hu Y, Li Z, et al. Overexpression of Roundabout4 predicts poor prognosis of primary glioma patients via correlating with microvessel density. J Neurooncol. 2015 May;123(1):161–9.

73. Jia ZZ, Gu HM, Zhou XJ, Shi JL, Li MD, Zhou GF, et al. The assessment of immature microvascular density in brain gliomas with dynamic contrast-enhanced magnetic resonance imaging. Eur J Radiol. 2015 Sep;84(9):1805–9.

74. Lüdemann L, Grieger W, Wurm R, Budzisch M, Hamm B, Zimmer C. Comparison of dynamic contrast-enhanced MRI with WHO tumor grading for gliomas. Eur Radiol. 2001 Jul;11(7):1231–41.

75. Falk A, Fahlström M, Rostrup E, Berntsson S, Zetterling M, Morell A, et al. Discrimination between glioma grades II and III in suspected low-grade gliomas using dynamic contrast-enhanced and dynamic susceptibility contrast perfusion

MR imaging: a histogram analysis approach. Neuroradiology. 2014 Dec;56(12):1031–8.

76. Jensen RL. Hypoxia in the tumorigenesis of gliomas and as a potential target for therapeutic measures. Neurosurg Focus. 2006 Apr;20(4):E24.

77. Nguyen TB, Cron GO, Mercier JF, Foottit C, Torres CH, Chakraborty S, et al. Preoperative Prognostic Value of Dynamic Contrast-Enhanced MRI-Derived Contrast Transfer Coefficient and Plasma Volume in Patients with Cerebral Gliomas. Am J Neuroradiol. 2015 Jan 1;36(1):63–9.

78. Yao Y, Kubota T, Takeuchi H, Sato K. Prognostic significance of microvessel density determined by an anti-CD105/endoglin monoclonal antibody in astrocytic tumors: Comparison with an anti-CD31 monoclonal antibody. Neuropathology. 2005 Sep;25(3):201–6.

Annexures

APPENDIX A

INFORMATION SHEET

Title Of The Study: The Diagnostic Utility Of Integration Of Dynamic Contrast Enhanced (Dce) And Dynamic Susceptibility Contrast(Dsc) Mr Perfusion Protocols, In Grading And Biological Behavior Characterisation Of Intraaxial Brain Tumors

Study number: SCT/IEC/940/AUGUST-2016

There is a clinical suspicion that you have brain tumor

Participant's name : Name, Date of Birth/Age (years): son/daughter of

---

There is a clinical suspicion that you have brain tumor, the severity (grading) of which needs to be assessed for choosing the best modality of management in your case. The Magnetic Resonance Imaging (MRI) investigation as a part of clinical evaluation helps to diagnose and plan the treatment of brain tumors.

The perfusion sequence is a type of MRI sequence used to assess the severity (grade) of brain tumors and is helpful for predicting the prognosis and the best modality of treatment to be undertaken in the patients.

There are two types of MR perfusion (named as dynamic susceptibility contrast and dynamic contrast enhanced) which can be done to assess the brain tumors. The integration of both these types of perfusion into the study , is likely to give a more complete assessment of brain tumor, compared to either of these perfusion used alone. This study is therefore designed to evaluate the role of combined MR perfusion in more accurate grading and prognostication of brain tumors. This study has the advantage of

likely providing more accurate brain tumor grading and therefore better directing the mode of treatment.

You are being requested to participate in this study which is likely to be more accurate in brain tumor grading and therefore in better individual patient management. Also, there is no additional risk anticipated as the investigation involves no additional dose of contrast compared to the existing institute protocol.

What is MRI and does it have any harmful effects?

MRI is an advanced imaging technique which uses certain waves and magnetic fields to image body part. It does not involve any ionizing radiation. Some patients may develop claustrophobia (Fear of closed spaces etc.) due to closed space and noise. This investigation is not to be done for patient with metallic implants, pacemakers. This MRI is being done as a part of clinical evaluation of your disease; however certain data from this study will be used for research purpose as part of this study.

If you take part what will you have to do?

This study will only analyze the results of the routinely ordered imaging investigations you will undergo for your illness. You will not be required to undergo any other additional investigation modality for this study.

Can you withdraw from this study after it starts?

Your participation in this study is entirely voluntary and you are also free to decide to withdraw permission to participate in this study. If you do so, this will not affect your usual treatment at this hospital in any way.

What will happen if you develop any study related injury?

This study only analyzes the results of the MRI investigation which you will be undergoing as part of your disease evaluation. Thus we do not expect any injury to happen to you but if you do develop any side effects or problems due to the study, these will be treated at this institute by the experienced team of medical professionals.

Will you have to pay for the study?

The study will only analyze the results of the investigations which you will undergo in natural process of the management of your disease process at this institute. No extra cost will be borne by you for this particular study.

What happens after the study is over?

If the study is found useful, the study will help better grade the brain tumors and better assess the mode of treatment to be chosen for the patients. The study may or may not be helpful to you directly.

Will your personal details be kept confidential?

The results of this study may be published in a medical journal but you will not be identified by name in any publication or presentation of results. However, your medical notes may be reviewed by people associated with the study, without your additional permission, should you decide to participate in this study.

If you have any further questions, please ask Dr. Virender Malik (tel: 9446522940) or email: drvm23@sctimst.ac.in

CONSENT FORM

TITLE OF THE STUDY: THE DIAGNOSTIC UTILITY OF INTEGRATION OF DYNAMIC CONTRAST ENHANCED(DCE) AND DYNAMIC SUSCEPTIBILITY CONTRAST(DSC) MR PERFUSION PROTOCOLS, IN GRADING AND BIOLOGICAL BEHAVIOR CHARACTERISATION OF INTRAAXIAL BRAIN TUMORS

Study number:

Participant's name: Date of Birth / Age (in years):

I_____

_____, son/daughter of _____ (Please tick boxes)

1. I Declare that I have read the above information provide to me regarding the study the diagnostic utility of integration of dynamic contrast enhanced and dynamic susceptibility contrast MR perfusion protocols, in grading and biological behavior characterization of intraaxial brain tumors and have clarified any doubts that I had. [ ]
2. I also understand that my participation in this study is entirely voluntary and that I am free to withdraw permission to continue to participate at any time without affecting my usual treatment or my legal rights [ ]
3. I understand that the study staff and institutional ethics committee members will not need my permission to look at my health records even if I withdraw from the trial. I agree to this access [ ]
4. I understand that my identity will not be revealed in any information released to third parties or published [ ]

5. I voluntarily agree to take part in this study [ ]
6. I received a copy of this signed consent form [ ]

Name: Signature: Date:

Name of witness: Relation to participant: Date:

I attest that the requirements for informed consent for the medical research project described in this form have been satisfied. I have discussed the research project with the participant and explained to him or her in nontechnical terms all of the information contained in this informed consent form, including any risks and adverse reactions that may reasonably be expected to occur. I further certify that I encouraged the participant to ask questions and that all questions asked were answered.

_____ _____

Name and Signature of Person Obtaining Consent

@ If there is any clarification sought by the participant : Please contact IEC member Secretary (study independent contact person), email: mala@sctimst.ac.in Tele No : 0471-2524234

APPENDIX B

SREE CHITRA TIRUNAL INSTITUTE FOR MEDICAL SCIENCES & TECHNOLOGY

PROFORMA

1. Case No :

2. Patient Particulars:

   a. Name:

   b. Hospital No:

   c. Age:

   d. Sex: M/F

   e. Address:

   f. Contact No:

   g. E-mail id :

   h. Date of admission :

   i. Date of Discharge:

3. Clinical Presentation:

4. Examination findings

5. MRI Findings

   a. Conventional MR

   b. MR Perfusion

   bi) Maximum rCBV value

bii) Maximum K-trans value

biii) Maximum Ve value

6. <u>Histopathological diagnosis</u> :

APPENDIX C:

ABBREVIATIONS:

DCE	:	Dynamic Contrast Enhanced
DSC	:	Dynamic Susceptibility Contrast
rCBV	:	Relative cerebral blood volume
Ve	:	Volume of extravascular extracellular space
Vp	:	Plasma Volume
k-trans	:	Transfer Constant
ASL	:	Arterial Spin Labeling
EES	:	Extravascular Extracellular Space
VEGF	:	Vascular Endothelial Growth Factor
BBB	:	Blood Brain Barrier
FPPM	:	First Pass Pharmacokinetic Model
AUC	:	Area Under Curve
IDH	:	Isocitrate Dehydrogenase
ROC	:	Receiver Operating Curve
MVD	:	Microvessel Density
LGN	:	Low Grade Neoplasm
HGN	:	High Grade Neoplasm
LGG	:	Low Grade Glioma
HGG	:	High Grade Glioma

PCNSL	:	Primary CNS Lymphoma
GBM	:	Glioblastoma
DMG	:	Diffuse Midline Glioma
AA	:	Anaplastic Astrocytoma
AODG	:	Anaplastic Oligodendroglioma

Plagiarism Checker X Originality Report

Similarity Found: 6%

Date: Saturday, July 28, 2018
Statistics: 223 words Plagiarized / 3776 Total words
Remarks: Low Plagiarism Detected - Your Document needs Optional Improvement.

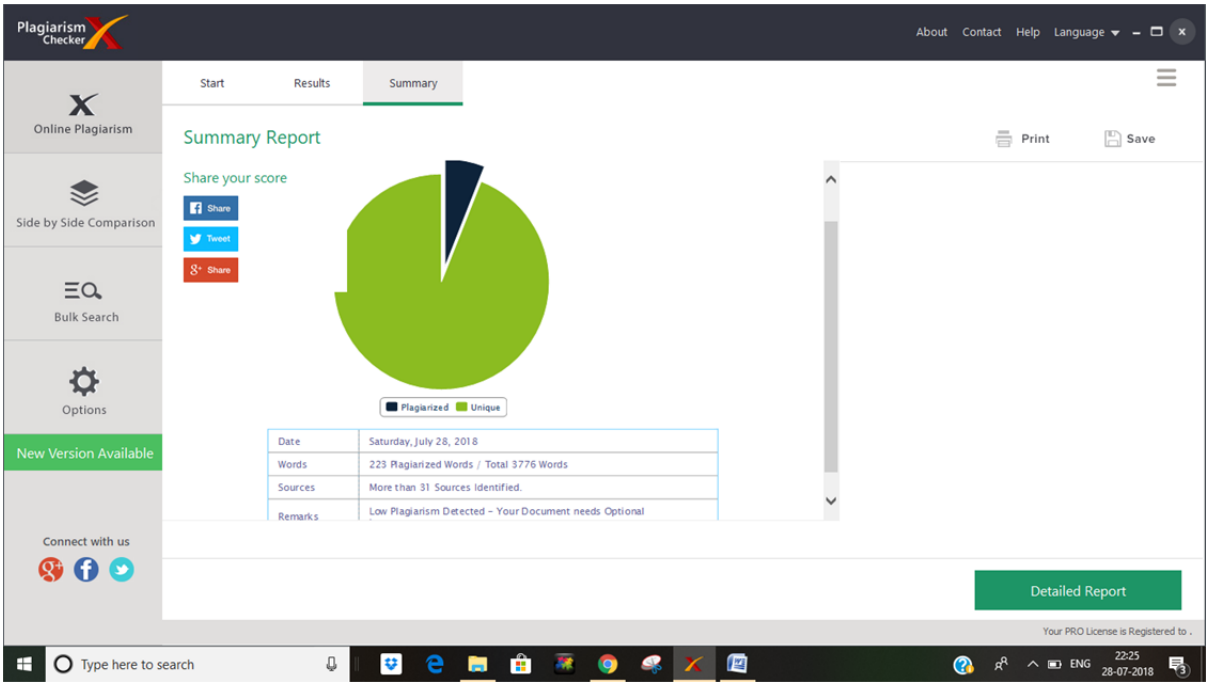

INTERNET SOURCES:

0% - https://radiopaedia.org/articles/mr-perf
0% - http://pubs.rsna.org/doi/full/10.1148/ra
0% - Empty
1% - https://www.ajronline.org/doi/full/10.22
1% - https://www.ajronline.org/doi/full/10.22
0% - http://www.ajronline.org/doi/full/10.221

0% - https://www.researchgate.net/profile/Rak
1% - https://www.ajronline.org/doi/full/10.22
1% - https://link.springer.com/article/10.118
2% - https://www.sciencedirect.com/science/ar
2% - https://www.sciencedirect.com/science/ar
0% - http://pubs.rsna.org/doi/10.1148/radiol.
2% - https://www.sciencedirect.com/science/ar
0% - https://www.sciencedirect.com/science/ar
1% - https://link.springer.com/article/10.118
0% - https://www.ncbi.nlm.nih.gov/pmc/article
0% - https://cancerimagingjournal.biomedcentr
2% - https://www.sciencedirect.com/science/ar
2% - https://www.sciencedirect.com/science/ar
0% - http://www.ajnr.org/content/38/6/1138
0% - https://www.sciencedirect.com/science/ar
2% - https://www.sciencedirect.com/science/ar
2% - https://www.sciencedirect.com/science/ar
0% - https://synapse.koreamed.org/Synapse/Dat
0% - http://www.medicinaoral.com/pubmed/medor
0% - http://www.nejm.org/doi/pdf/10.1056/NEJM
0% - https://oncohemakey.com/epidemiology-of-
0% - https://springerplus.springeropen.com/ar
2% - https://www.sciencedirect.com/science/ar
1% - https://link.springer.com/article/10.118
0% - https://alzres.biomedcentral.com/article
0% - http://www.atsjournals.org/doi/full/10.1
0% - https://en.wikipedia.org/wiki/Pancreatic
0% - http://mcmed.us/downloads/146018370033(a
0% - https://link.springer.com/article/10.100
0% - http://journals.plos.org/plosone/article
0% - https://cancerimagingjournal.biomedcentr
0% - https://www.researchgate.net/profile/Ann
0% - https://www.sciencedirect.com/science/ar
0% - https://www.hindawi.com/journals/bmri/20
1% - https://link.springer.com/article/10.118
0% - https://www.researchgate.net/profile/Ho_
1% - https://www.ajronline.org/doi/full/10.22
0% - https://rd.springer.com/chapter/10.1007/

APPENDIX D:

EXCEL SHEET

S.No	AGE[years	SEX	K-TRANS	Ve	rCBV	MVD	HPE	IDH status	Tissue sa	Side	Side
1	42	Male	0.120	0.209	6.63	133.17	GBM	M	DE	PT	L
2	44	Male	0.204	0.436	4.14	59.95	GBM	W	DE	I	L
3	65	Female	0.282	0.201	12.09	141.52	GBM	W	DE	PT	R
4	65	Male	0.154	0.249	5.19	142.51	GBM	W	DE	I	L
5	65	Male	0.216	0.365	3.66	45.21	GBM	W	DE	F	R
6	24	Male	0.080	0.173	7.18	127.76	GBM	W	DE	F	L
7	32	Male	1.176	0.182	10.56	229.98	GBM	M	DE	F	R
8	65	Female	0.322	0.271	5.22	121.38	GBM	W	DE	IF	R
9	59	Male	0.564	0.451	9.01	304.17	GBM	W	DE	F	R
10	75	Male	0.288	0.406	3.63	81.60	GBM	W	B	T	L
11	54	Male	0.096	1.000	4.35	89.43	GBM	W	DE	F	R
12	42	Female	0.068	0.137	2.73	228.50	GBM	W	DE	F	L
13	66	Male	0.112	0.212	4.82	113.02	GBM	W	DE	F	R
14	54	Female	0.034	0.087	0.58	53.07	AA	M	DE	F	R
15	29	Male	0.052	0.013	1.42	68.30	AA	W	DE	F	L
16	42	Male	0.336	0.055	2.24	122.85	AA	W	DE	F	L
17	37	Female	0.568	0.067	1.94	82.56	AA	M	B	F	R
18	44	Male	0.688	1.000	4.82	108.60	AA	M	DE	F	L
19	29	Male	0.493	0.057	4.63	116.95	AA	W	DE	T	L
20	45	Male	0.060	0.034	1.89	93.37	AA	W	DE	F	L
21	27	Male	0.070	0.007	1.00	42.26	AA	M	DE	T	L
22	41	Male	0.381	0.066	7.86	182.31	AA	W	DE	F	R
23	37	Female	0.240	0.162	3.46	211.30	AA	M	DE	F	R
24	46	Female	0.064	0.009	1.16	149.88	AA	M	DE	I	R
25	40	Female	0.495	0.112	3.17	221.13	AA	W	DE	F	L
26	32	Female	0.064	0.023	1.17	51.59	AA	M	DE	F	R
27	43	Male	0.068	0.044	3.45	74.20	AA	M	DE	F	R
28	21	Female	0.336	0.205	6.89	108.60	AA	W	DE	FO	L
29	52	Male	0.072	0.175	6.08	85.50	AA		DE	F	R
30	40	Male	0.464	0.037	4.96	95.82	ADOG	M	DE	F	R
31	31	Male	0.048	0.008	1.54		ADOG	M	DE	F	R
32	40	Male	0.128	0.026	4.41	168.55	ADOG	M	DE	F	L
33	54	Male	0.056	0.039	1.80	127.27	ADOG	M	DE	T	L
34	46	Female	0.257	0.352	10.79	245.21	ADOG	M	DE	F	R
35	37	Female	0.128	0.020	1.21	97.30	ADOG	M	DE	FI	R
36	39	Female	0.033	0.047	1.32	49.63	ADOG	M	DE	F	R
37	57	Female	0.208	0.088	7.04	117.44	ADOG	M	DE	F	L
38	41	Female	0.056	0.037	0.97	52.58	DA	M	DE	T	L
39	45	Female	0.072	0.025	1.28		DA		DE	FT	L
40	33	Female	0.080	0.012	0.70		DA			F	R
41	41	Female	0.032	0.024	1.13		DA			F	R
42	32	Male	0.048	0.021	1.25		DA			T	R
43	49	Female	0.048	0.012	0.90		DA			F	L
44	36	Male	0.048	0.015	1.06		DA			P	R
45	40	Female	0.032	0.015	1.00		DA			F	L
46	60	Male	0.252	0.821	1.04		PONSL		DE	F	R
47	60	Female	0.224	0.266	10.32		PONSL		B	BG	R
48	46	Male	0.137	0.463	6.19		PONSL	M	B	THALAMU	L
49	29	Male	0.446	0.046	4.17		DMG		B	THALAMUS	R
50	20	Male	0.264	0.454	3.93	54.05	DMG		B	THALAMUS	R
51	25	Female	0.080	0.439	5.04	37.35	DMG		B	THALAMUS	R
52	37	Male	0.352	0.228	12.34	145.94	DMG		B	THALAMUS	R

ABBREVIATIONS FOR EXCEL SHEET

k-trans	:	Transfer Constant
Ve	:	Volume of extravascular extracellular space
rCBV	:	Relative cerebral blood volume
IDH	:	Isocitrate Dehydrogenase
MVD	:	Microvessel Density
DA	:	Diffuse Astrocytoma
AA	:	Anaplastic Astrocytoma
AODG	:	Anaplastic Oligodendroglioma
PCNSL	:	Primary CNS Lymphoma
GBM	:	Glioblastoma
DMG	:	Diffuse Midline Glioma

APPENDIX E:

IEC permission:

श्री चित्रा तिरुनाल आयुर्विज्ञान और प्रौद्योगिकी संस्थान, त्रिवेन्द्रम
तिरुवनन्तपुरम - ६९५०११, केरल, इंडिया
SREE CHITRA TIRUNAL INSTITUTE FOR MEDICAL SCIENCES AND TECHNOLOGY, TRIVANDRUM
Thiruvananthapuram - 695 011, Kerala, India
(An Institute of National Importance under Govt. of India)
Grams : Chitramet, Phone : +91-471-2443152, Fax : +91-471-2550728 / 2446433, E-mail : sct@sctimst.ac.in, Website : www.sctimst.ac.in

Institutional Ethics Committee
IEC Regn No. ECR/189/Inst/KL/2013)

SCT/IEC/940/AUGUST-2016 *07.10.2016*

Dr. Virender Malik
Senior Resident
Department of IS & IR
SCTIMST, Thiruvananthapuram

Dear Dr. Virender Malik,

The Institutional Ethics Committee reviewed and discussed your application to conduct the study entitled "THE DIAGNOSTIC UTILITY OF INTEGRATION OF DYNAMIC CONTRAST ENHANCED (DCE) AND DYNAMIC SUSCEPTIBILITY CONTRAST (DSC) IN MR PERFUSION PROTOCOLS, IN GRADING AND BIOLOGICAL BAHAVIOR CHARACTERISATION OF INTRAAXIAL BRAIN TUMORS" (IEC/940) on 20th August, 2016.

The following documents were reviewed:

Original submission

1. *Covering letter addressed to the Chairperson, IEC, SCTIMST, dated 25.07.2016 with check list*
2. *TAC Approval Letter*
3. *IEC Application Form*
4. *Project Proposal*
5. *Proforma*
6. *Informed Consent Forms in English and Malayalam*
7. *Patient Information Sheets in English and Malayalam*
8. *CV of Principal Investigator and Co- Investigators*

Revised submission

1. *Covering letter addressed to the Chairperson, IEC, SCTIMST, dated 04.10.2016 with check list*
2. *IEC Application Form*
3. *TAC Approval Letter*
4. *Project Proposal*
5. *Proforma*
6. *Informed Consent Forms in English and Malayalam*
7. *Patient Information Sheets in English and Malayalam*
8. *CV of Principal Investigator and Co- Investigators*